Advances in Polyolefins 2009

Quantification of the Macromolecular/Nanoscale Topology using Small Angle Neutron and X-ray Scattering

Greg Beaucage
Ram Ramachandran, Durgesh Rai, Amit Kulkarni (Sabic Plastics)
Department of Chemical and Materials Engineering
University of Cincinnati

UNIVERSITY OF Cincinnati

Quantification of the Macromolecular/Nanoscale Topology using Small Angle Neutron and X-ray Scattering

Greg Beaucage
Ram Ramachandran, Durgesh Rai, Amit Kulkarni (Sabic Plastics)
Department of Chemical and Materials Engineering
University of Cincinnati

V. Galiatsatos, D. McFaddin, J. Merrick-Mack

LyondellBasell Corporation (Equistar)

lyondellbasell

Advances in Polyolefins 2009

Quantification of the Macromolecular/Nanoscale Topology using Small Angle Neutron and X-ray Scattering

Greg Beaucage
Ram Ramachandran, Durgesh Rai, Amit Kulkarni (Sabic Plastics)
Department of Chemical and Materials Engineering
University of Cincinnati

HFIR
Oak Ridge National Laboratory

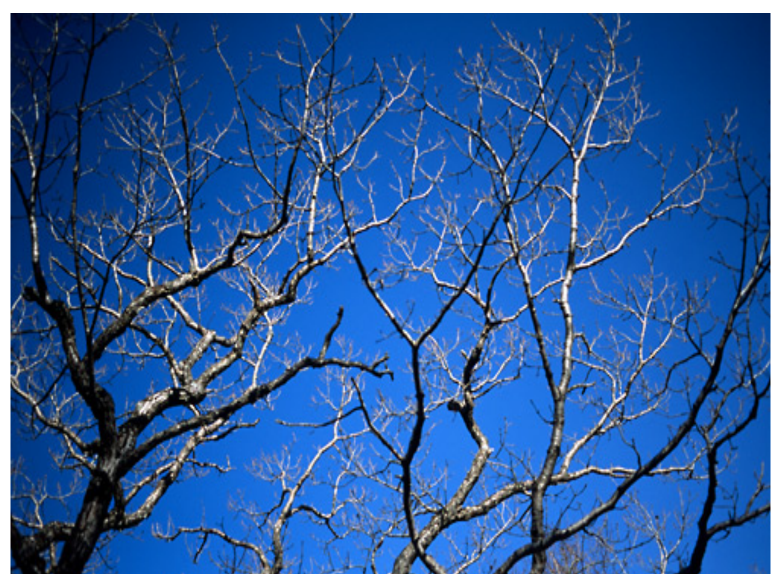

IPNS, Argonne
National Laboratory

NIST
Center for Neutron Scattering

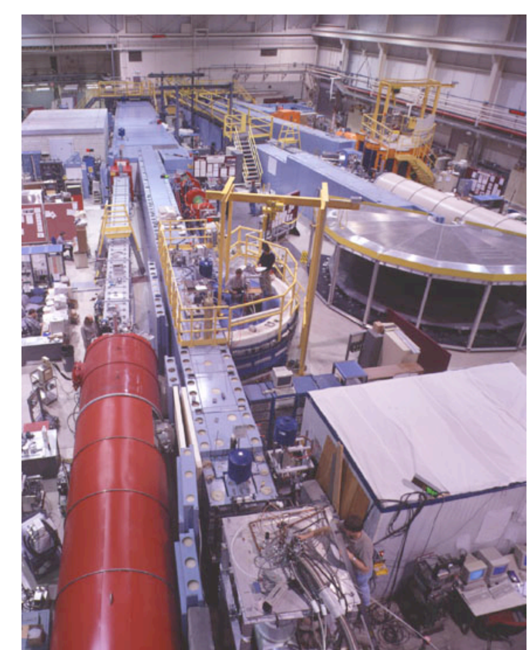

Randomly Branched Structures

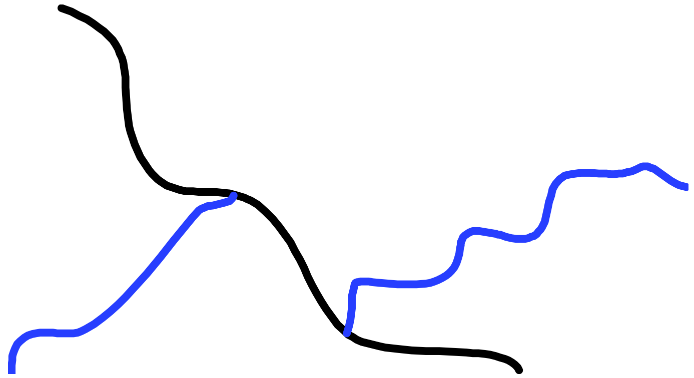

Long Chain Branching

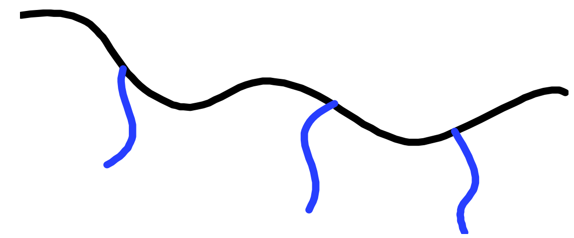

Short Chain Branching

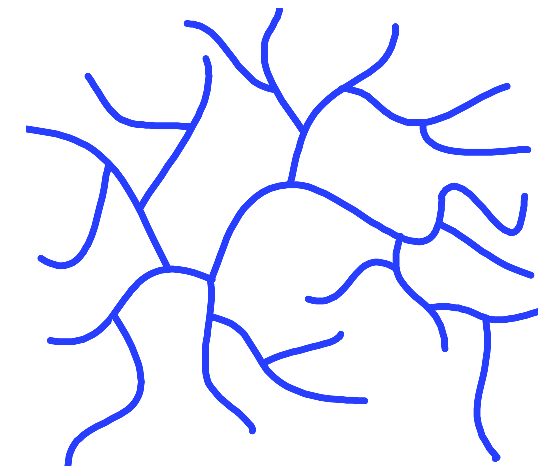

Hyperbranched

Controlled Branched Structures

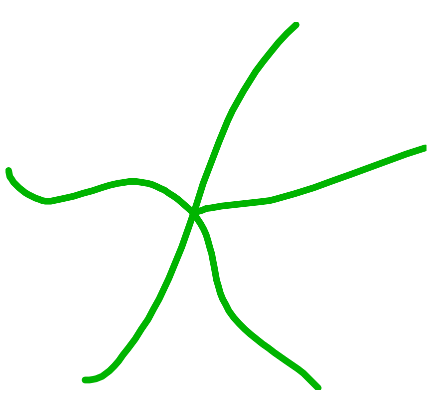

Star

Comb

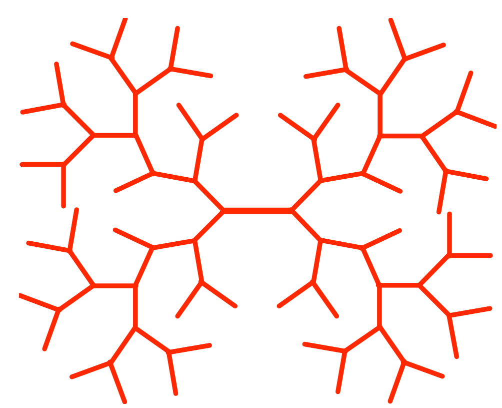

Dendrimer

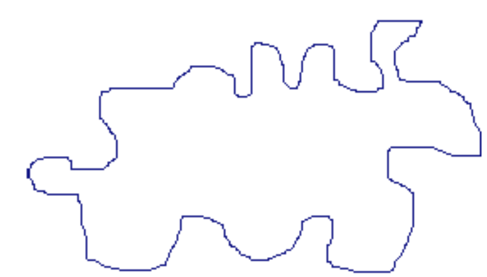

Cyclic

Randomly Branched Structures

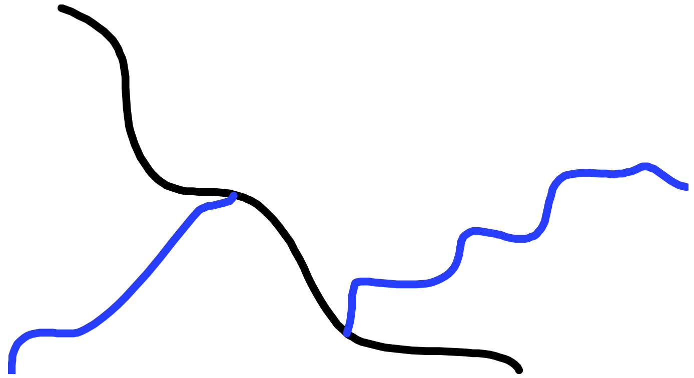

Long Chain Branching

Branch content of metallocene polyethylene Ramachandran R, Beaucage G, Kulkarni AS, McFaddin D, Merrick-Mack J, Galiatsatos V *Macromolecules*, **42** 4746-4750 (2009).

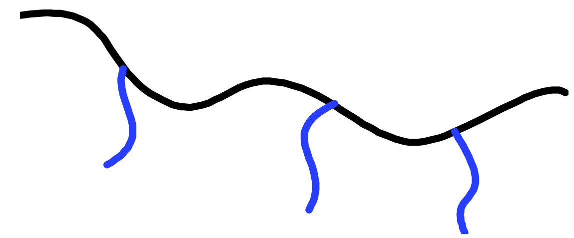

Short Chain Branching

Persistence Length of Short-Chain Branched Polyethylene Ramachandran R, Beaucage G, Kulkarni AS, McFaddin D, Merrick-Mack J, Galiatsatos V *Macromolecules* **41** 9802-9806 (2008).

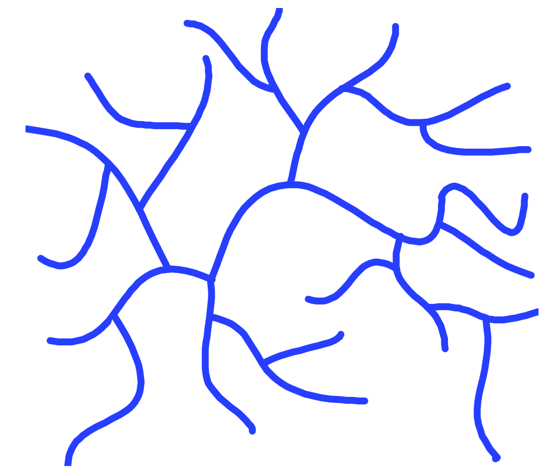

Hyperbranched

Investigating the molecular architecture of hyperbranched polymers using small angle neutron scattering. Kulkarni AS, Beaucage G *Macromolecular Rapid Comm*. **28**, 1312-1316 (2007).

Controlled Branched Structures

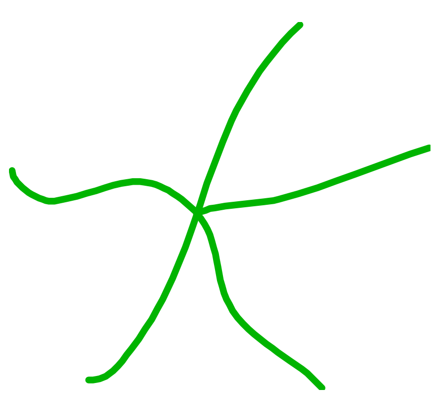

Star

Comb

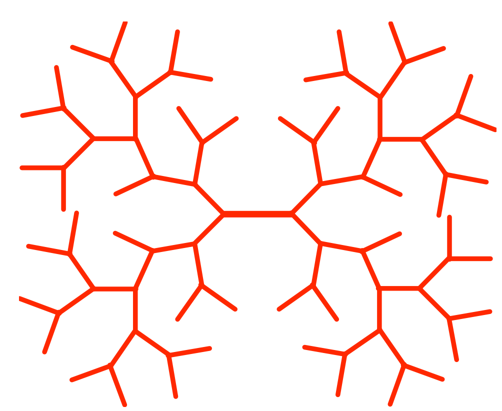

Dendrimer

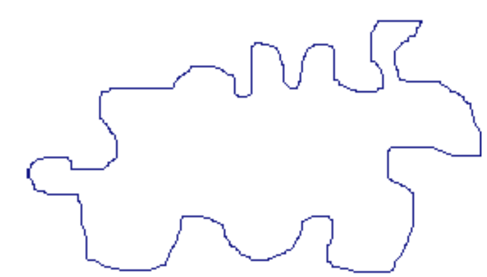

Cyclic

Several Papers in Preparation (2009).

Randomly Branched Structures

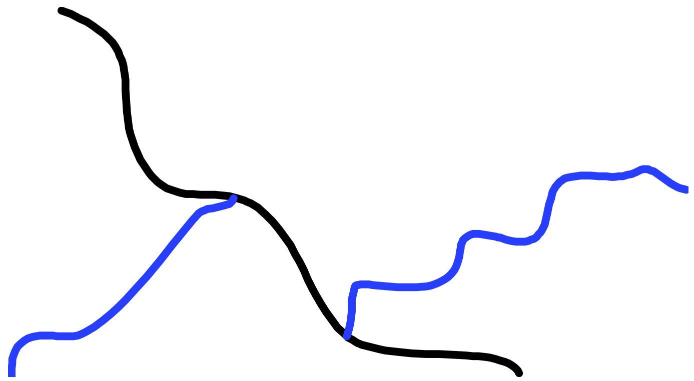

Long Chain Branching

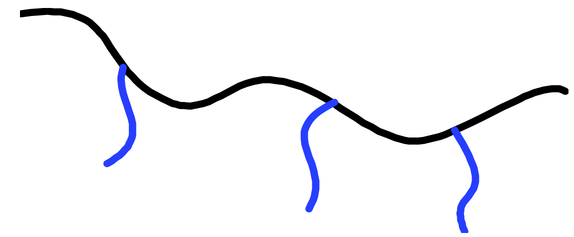

Short Chain Branching

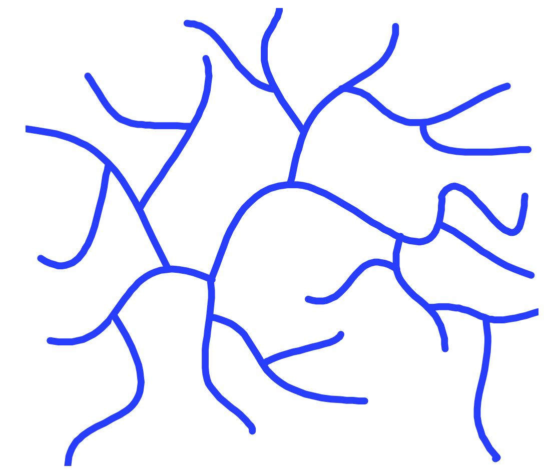

Hyperbranched

Nano-scale Aggregates

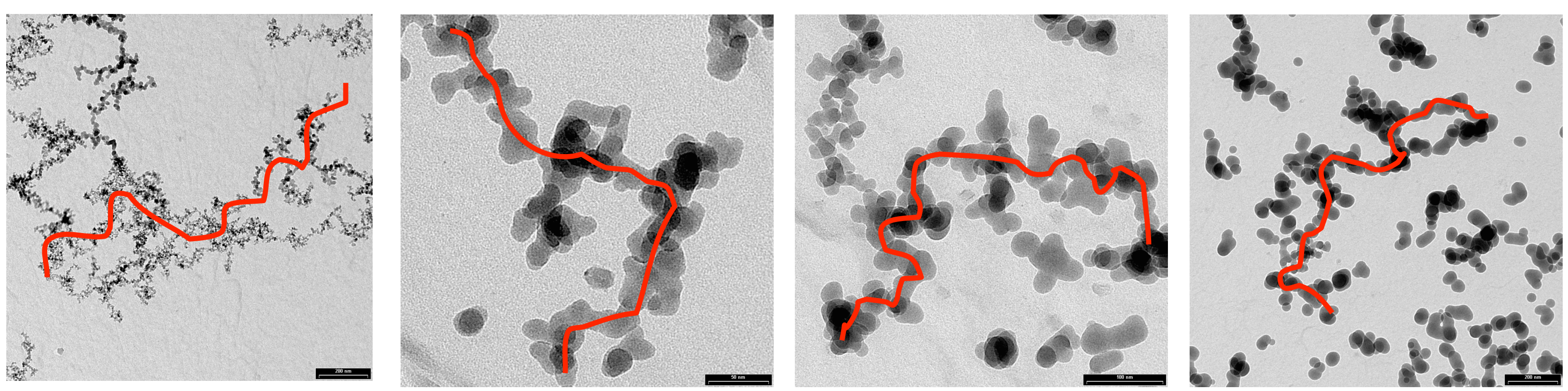

In situ study of aggregation of soot particles in an acetylene flame by small-angle x-ray scattering Sztucki M, Narayanan T, Beaucage G *J. Appl. Phys.* **101** 114304 (2007)

Biomolecules

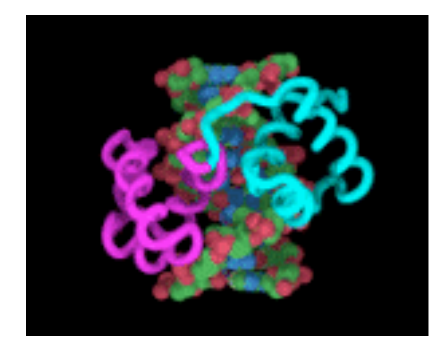

Towards resolution of ambiguity for the unfolded state. Beaucage G *Biophysical J.* **95** 503-509 (2008).

The SAXS Experiment

Source Collimination Sample Detector

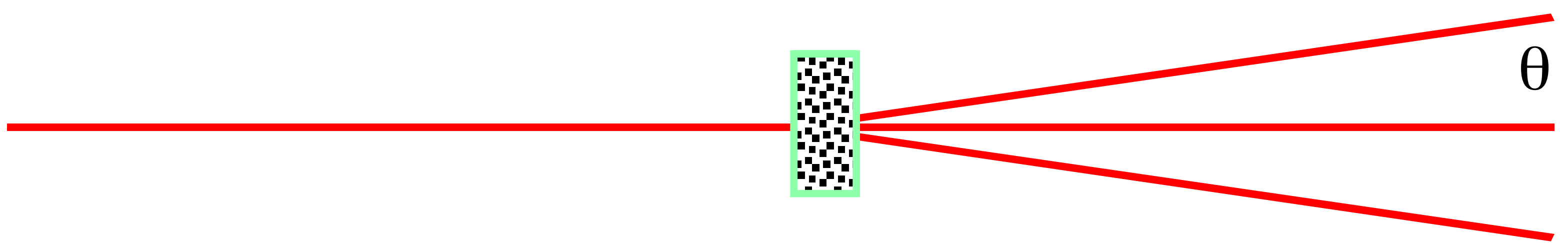

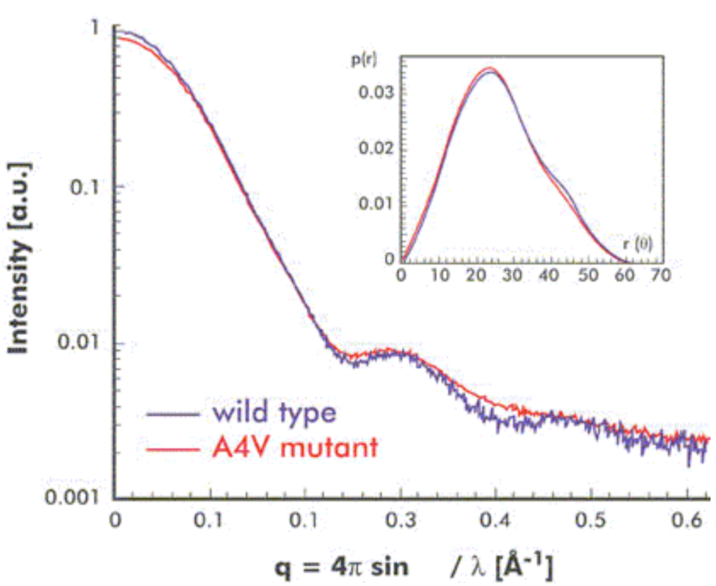

$$q = \frac{4\pi}{\lambda}\sin\left(\frac{\theta}{2}\right) = \frac{2\pi}{d}$$

$$I(q) = Nn_e^2 = A^2(q)$$

1-meter

SAXS

30-meter

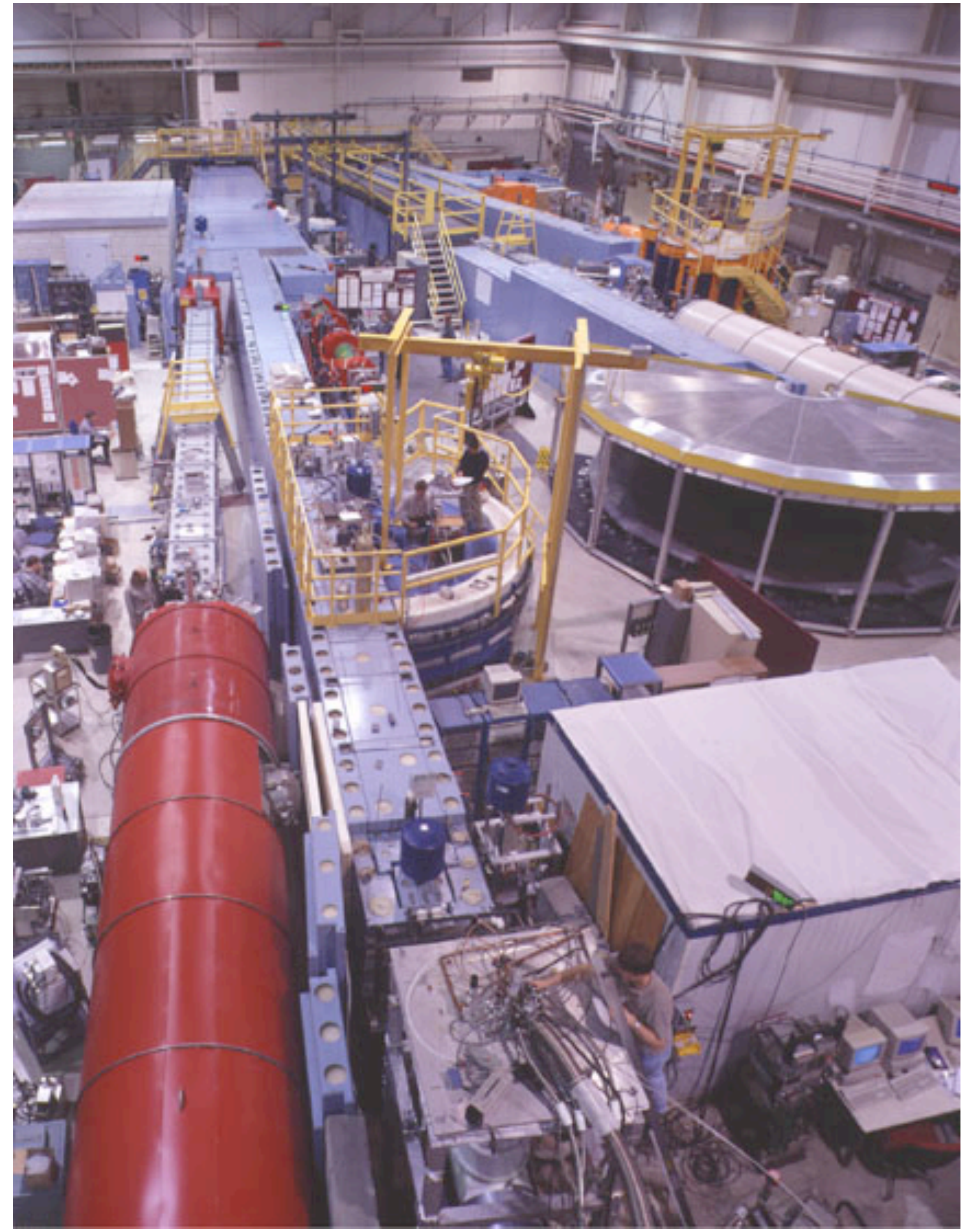

SANS

1-meter

SAXS

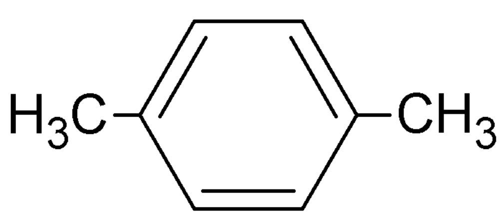

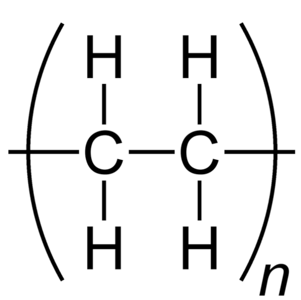

30-meter

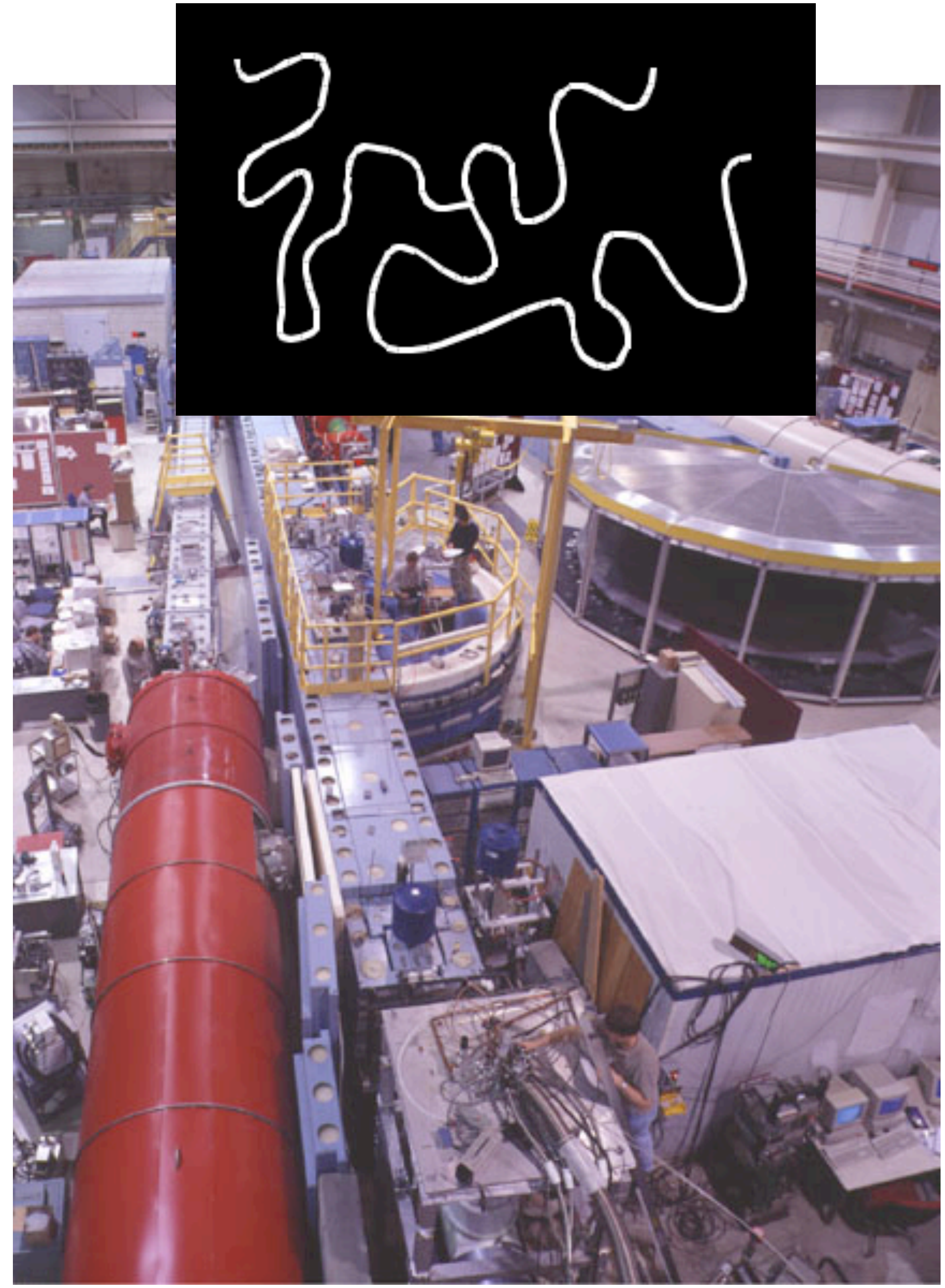

SANS

Fractal Hierarchical Structure
Long Chain Branched Hydrogenated Polybutadiene (Polyethylene)

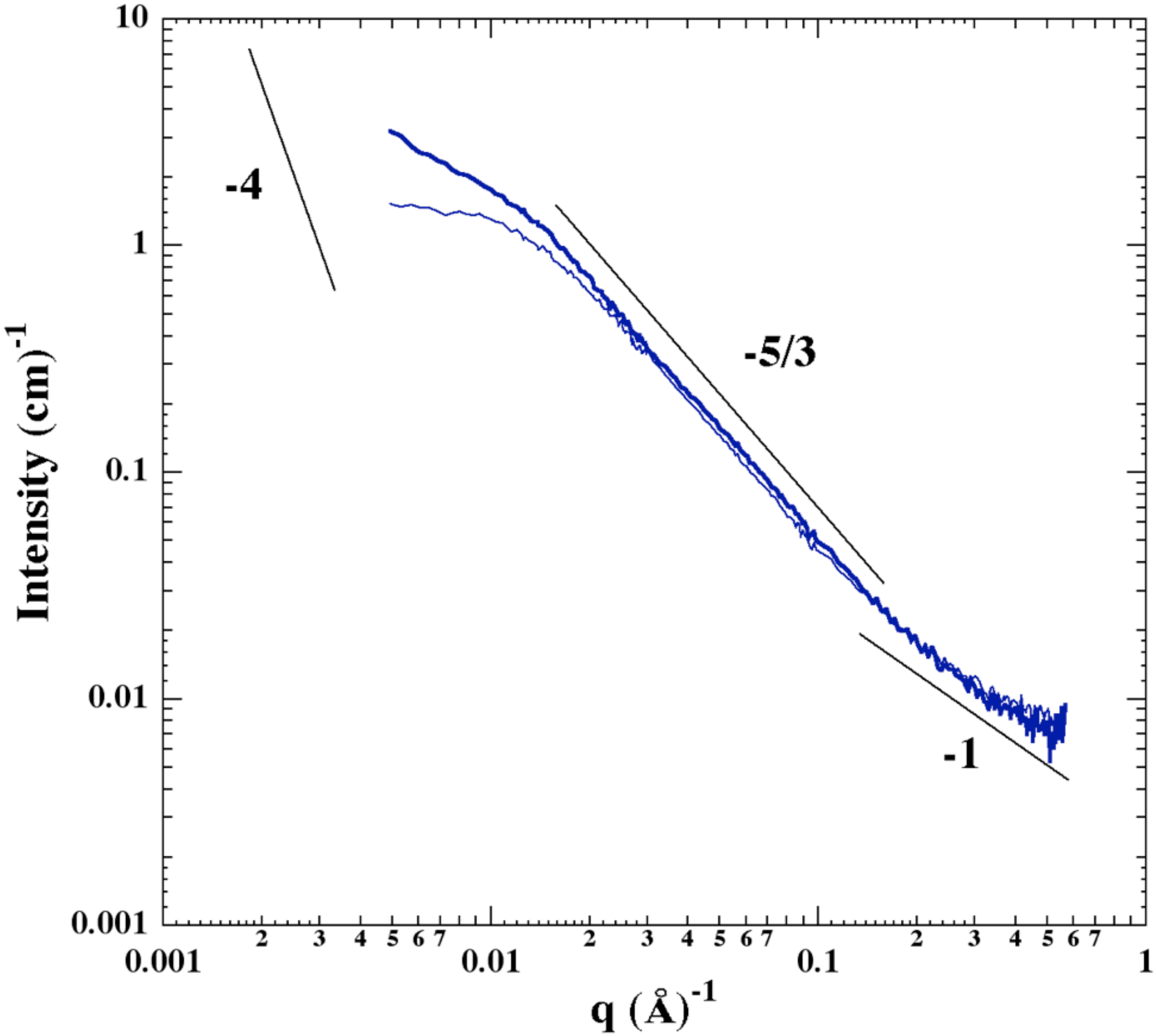

Fractal Hierarchical Structure
Long Chain Branched Hydrogenated Polybutadiene
(Polyethylene)

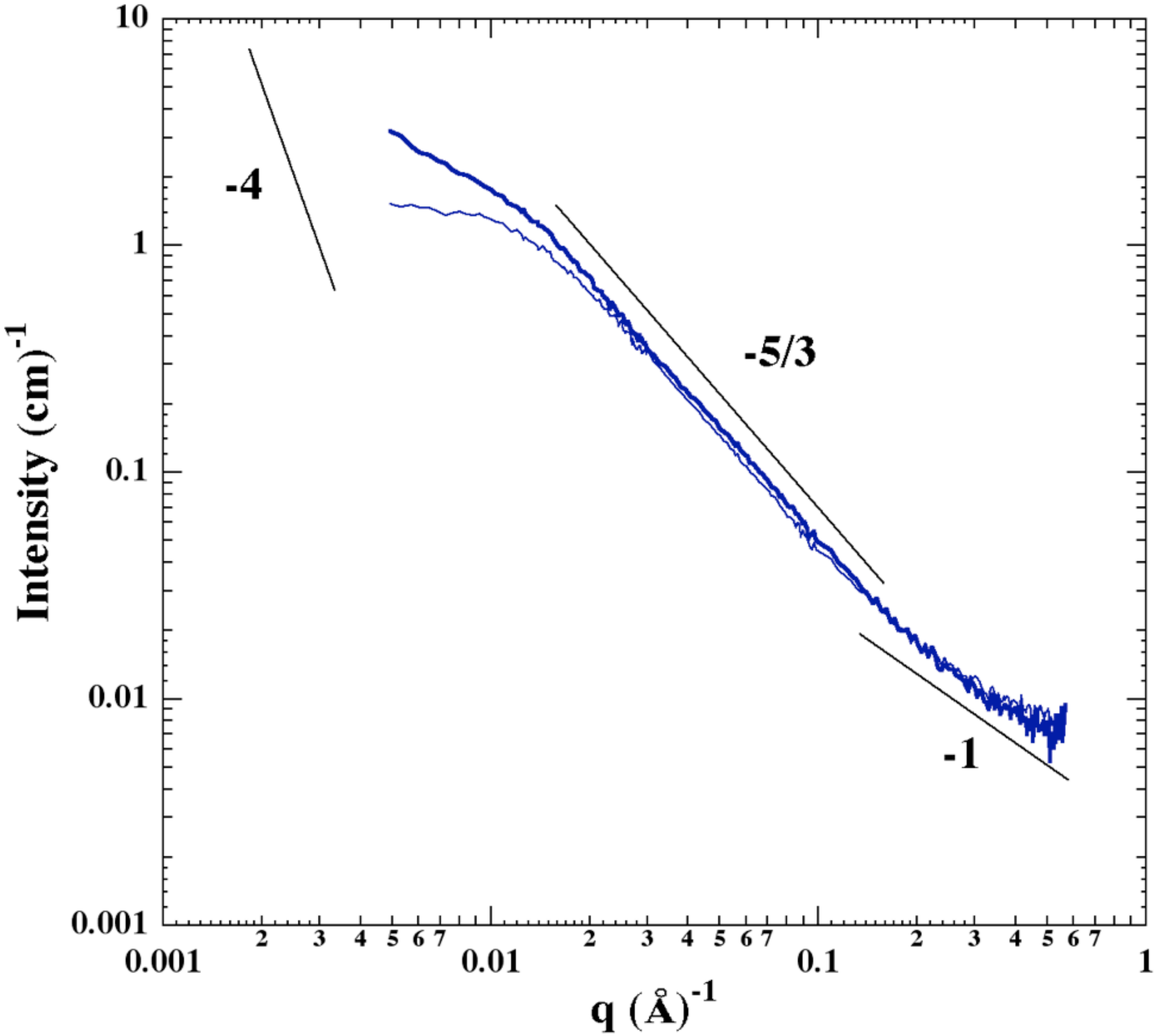

$z \sim (R/l_K)^{df}$

$I \sim z$

$q \sim 1/d \sim (l_K/R)$

$I(q) \sim q^{df}$

Fractal Hierarchical Structure
Long Chain Branched Hydrogenated Polybutadiene (Polyethylene)

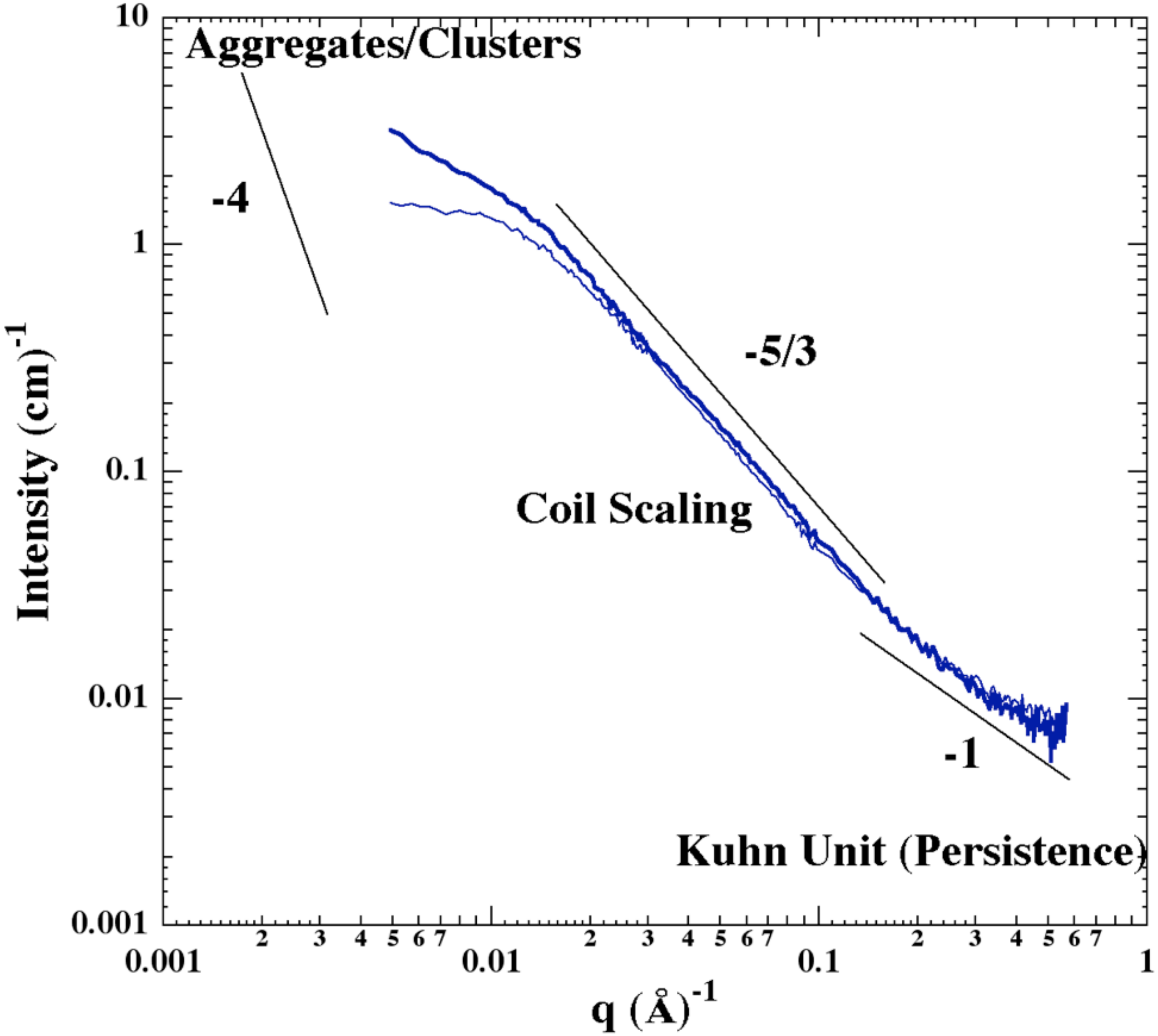

$$I(q) \sim q^{df}$$

Unified Function Builds Hierarchy Through Structural Levels

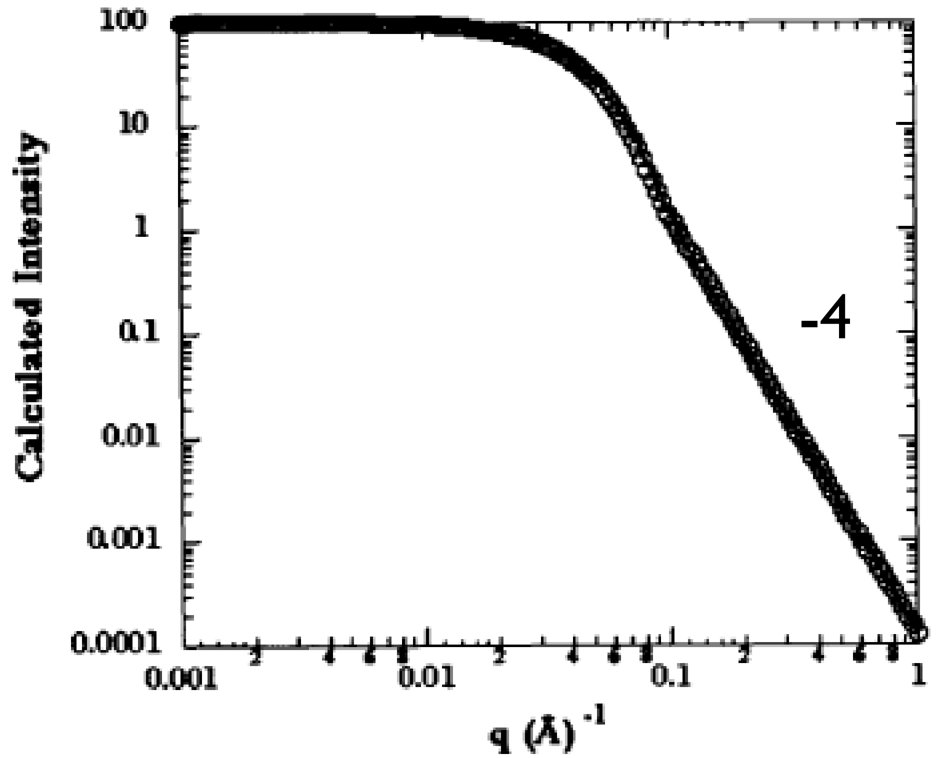

Fig. 11. Calculated scattering (○) from polydisperse spheres with Porod surfaces (power law − 4). The solid line follows equation (24) with $R_g = 39.495$ Å as calculated and $P = 4$, $G = 100$ cm^{-1} (fixed in the sphere calculation) and $B = 0.000\,127\,52$ from Porod's law.

Porod Regime

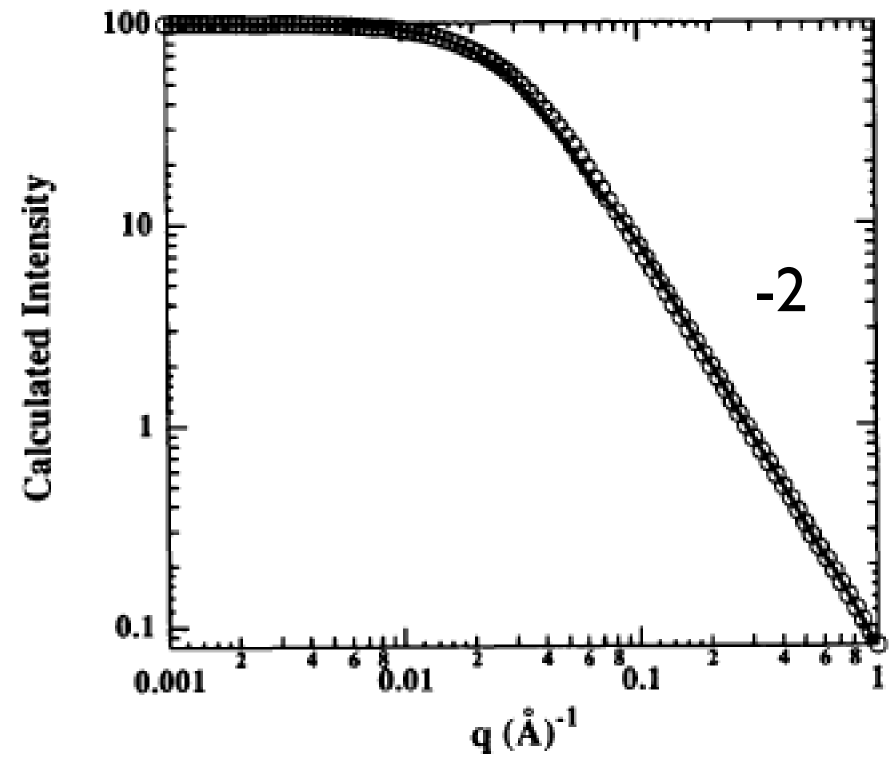

Fig. 10. Log–log plot of Debye equation (○) and equation (24) (solid line). For the Debye equation, $R_g = 50$ Å and $A = 100$ cm^{-1}. For the unified equation, (24), all parameters are fixed. $R_g = 50$ Å, $G = 100$ cm^{-1}, $P = 2$ (the Debye equation represents a mass fractal with $d_f = 2$) and $B = 0.08 = 2G/R_g^2$ from equation (30).

Fractal Regime

Beaucage G *J. Appl. Cryst.* **28** 717-728 (1995).

Unified Function Builds Hierarchy Through Structural Levels

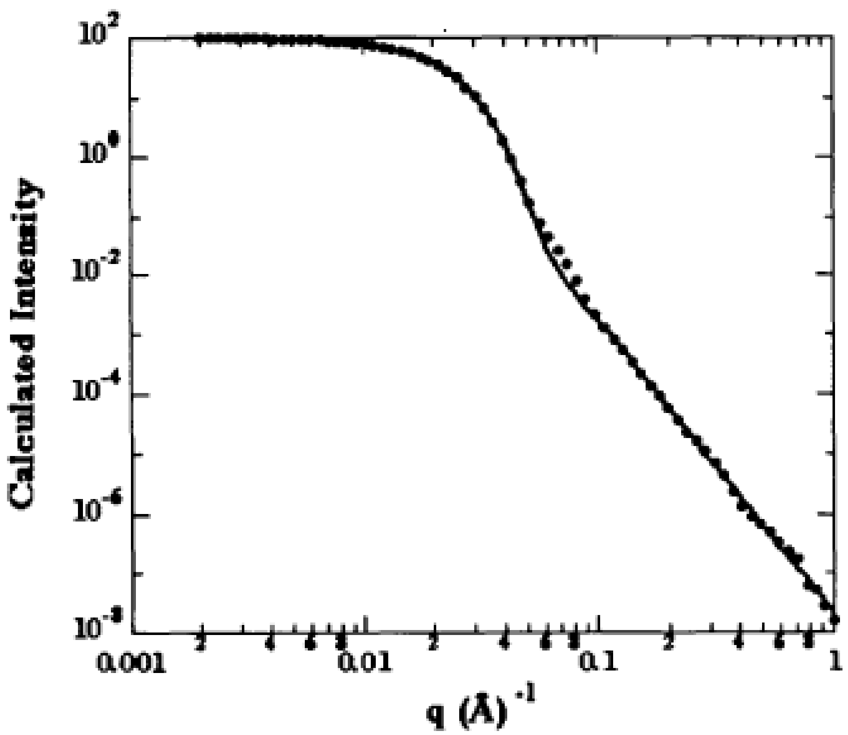

Fig. 12. Calculated scattering curve for an ellipsoid of revolution with a spherical shell of lower electron density, 0.36 of core, with major : minor axis ratio of 4 : 1 and minor axis of $R = 50$ Å and 60 Å for the core and shell, respectively. Equation (24) is calculated using $R_g = 87.9$, $G = 100$ cm^{-1}, $P = 4.91$ and $B = 1.99 \times 10^{-8}$. The mismatch at $q = 0.07$ Å^{-1} is due to a residual Fourier peak that has not been averaged out and that would normally not appear in experimental data for a diffuse interface.

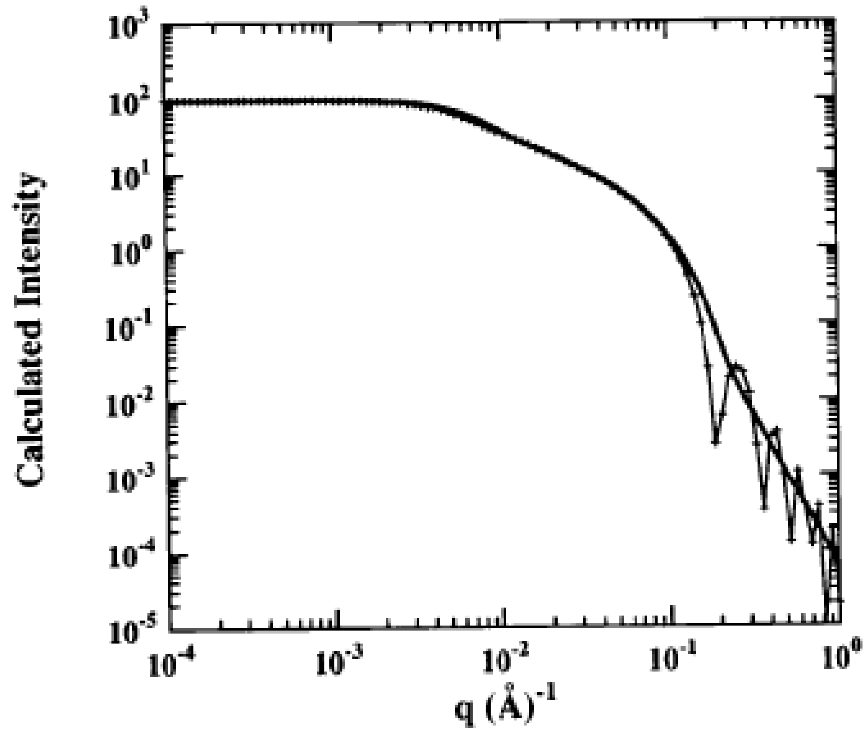

Fig. 13. Calculated scattering curve [Guinier & Fournet, 1955, p. 19, equation (33)] from randomly oriented rods of diameter 40 Å and length 800 Å (+). $I(0)$ is fixed at 100. The calculated scattering curve using equation (28) is shown by the bold line, and $G = 100$, $R_g = 231.4$ Å, $P = 1$, $B = 0.393$, $R_{sub} = R_s = 17.3$ Å, $G_s = 0.111$, $B_s = 6.25 \times 10^{-5}$ and $P_s = 4$ as discussed in the text. High-q oscillations in the + curve are due to poor averaging in the calculation.

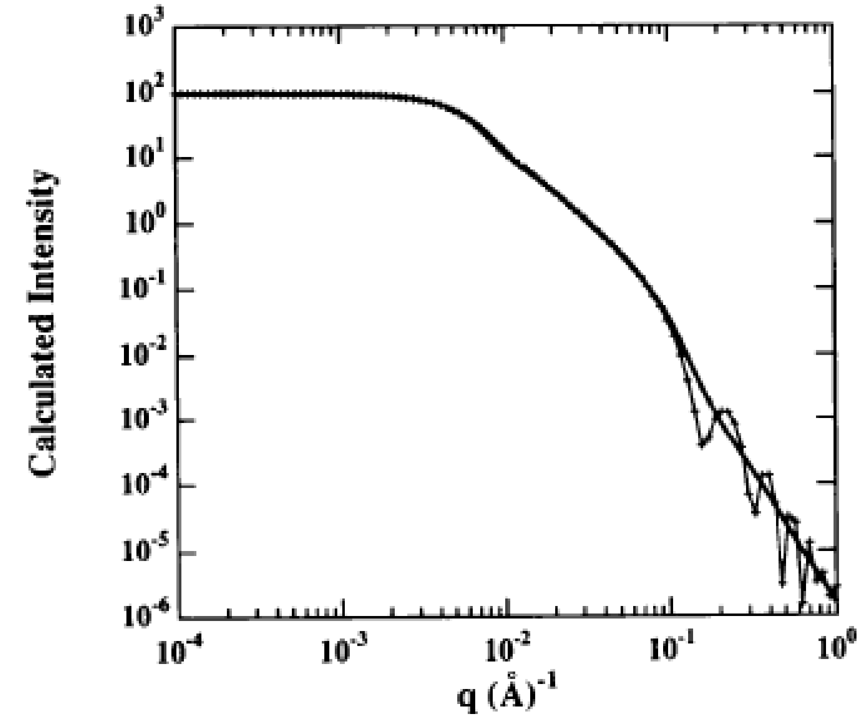

Fig. 14. Calculated scattering curve [Guinier & Fournet, 1955, p. 19, equation (33)] from randomly oriented disc-like lamellae of thickness 40 Å and diameter 800 Å (+). $I(0)$ is fixed at 100. The calculated scattering curve using equation (28) is shown by the bold line, and $G = 100$, $R_g = 283.1$ Å, $P = 2$, $B = 1.25 \times 10^{-3}$, $R_{sub} = R_s = 20$ Å, $G_s = 2.78 \times 10^{-4}$, $B_s = 1.56 \times 10^{-6}$ and $P_s = 4$ as discussed in the text. High-q oscillations in the + curve are due to poor averaging in the calculation.

Beaucage G *J. Appl. Cryst.* **28** 717-728 (1995).

Unified Function Builds Hierarchy Through Structural Levels

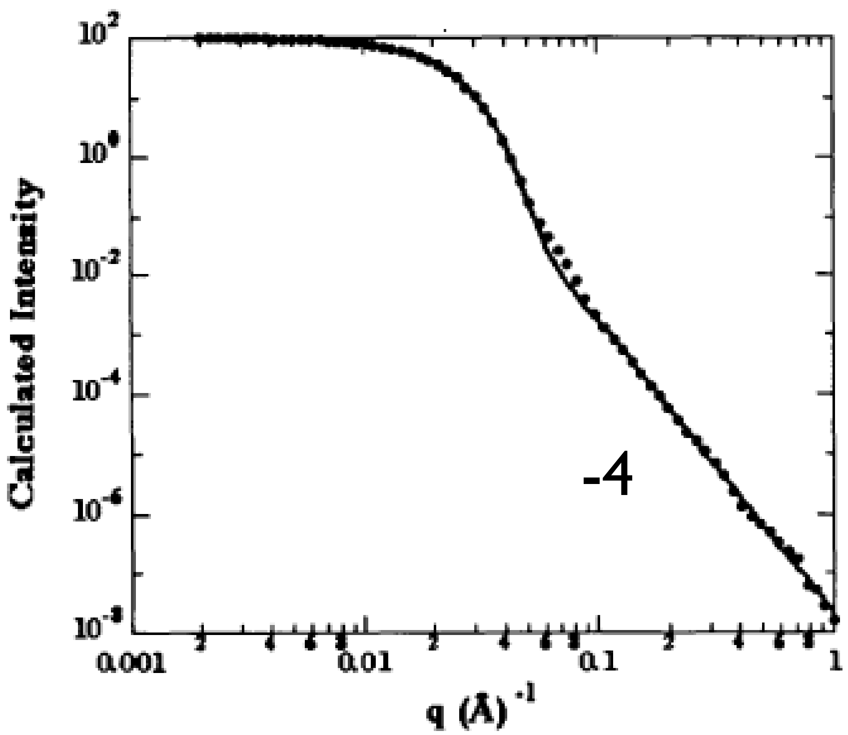

Fig. 12. Calculated scattering curve for an ellipsoid of revolution with a spherical shell of lower electron density, 0.36 of core, with major : minor axis ratio of 4 : 1 and minor axis of $R = 50$ Å and 60 Å for the core and shell, respectively. Equation (24) is calculated using $R_g = 87.9$, $G = 100$ cm^{-1}, $P = 4.91$ and $B = 1.99 \times 10^{-8}$. The mismatch at $q = 0.07$ Å^{-1} is due to a residual Fourier peak that has not been averaged out and that would normally not appear in experimental data for a diffuse interface.

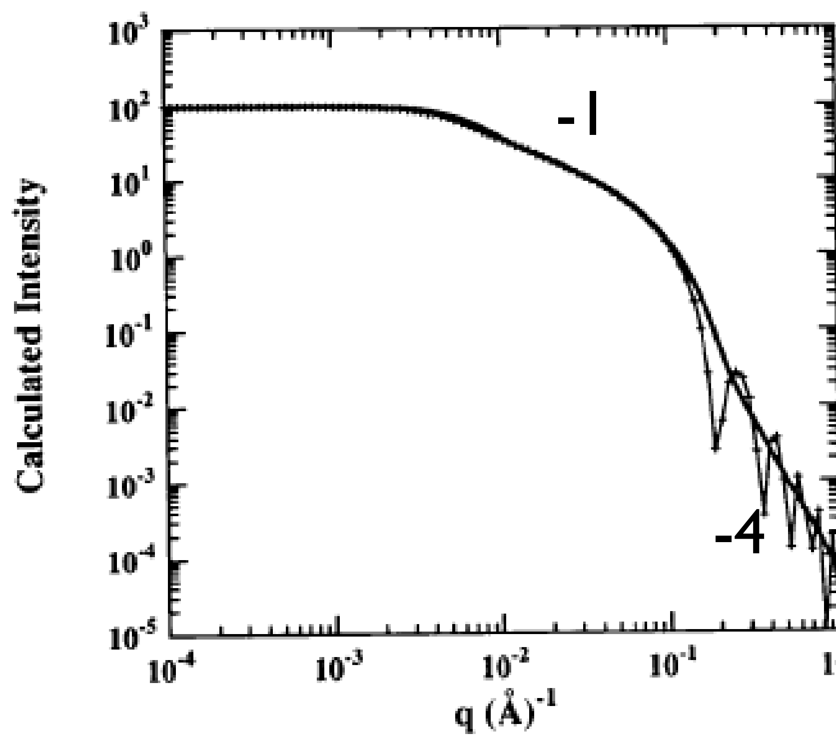

Fig. 13. Calculated scattering curve [Guinier & Fournet, 1955, p. 19, equation (33)] from randomly oriented rods of diameter 40 Å and length 800 Å (+). $I(0)$ is fixed at 100. The calculated scattering curve using equation (28) is shown by the bold line, and $G = 100$, $R_g = 231.4$ Å, $P = 1$, $B = 0.393$, $R_{sub} = R_s = 17.3$ Å, $G_s = 0.111$, $B_s = 6.25 \times 10^{-5}$ and $P_s = 4$ as discussed in the text. High-q oscillations in the + curve are due to poor averaging in the calculation.

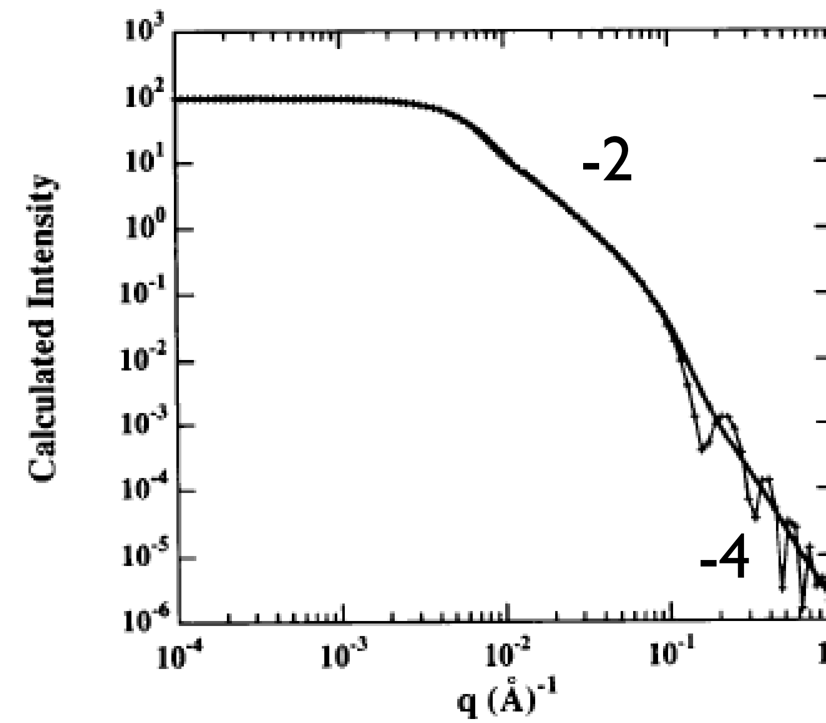

Fig. 14. Calculated scattering curve [Guinier & Fournet, 1955, p. 19, equation (33)] from randomly oriented disc-like lamellae of thickness 40 Å and diameter 800 Å (+). $I(0)$ is fixed at 100. The calculated scattering curve using equation (28) is shown by the bold line, and $G = 100$, $R_g = 283.1$ Å, $P = 2$, $B = 1.25 \times 10^{-3}$, $R_{sub} = R_s = 20$ Å, $G_s = 2.78 \times 10^{-4}$, $B_s = 1.56 \times 10^{-6}$ and $P_s = 4$ as discussed in the text. High-q oscillations in the + curve are due to poor averaging in the calculation.

Beaucage G *J. Appl. Cryst.* **28** 717-728 (1995).

Fractal Hierarchical Structure
$P = d_f$

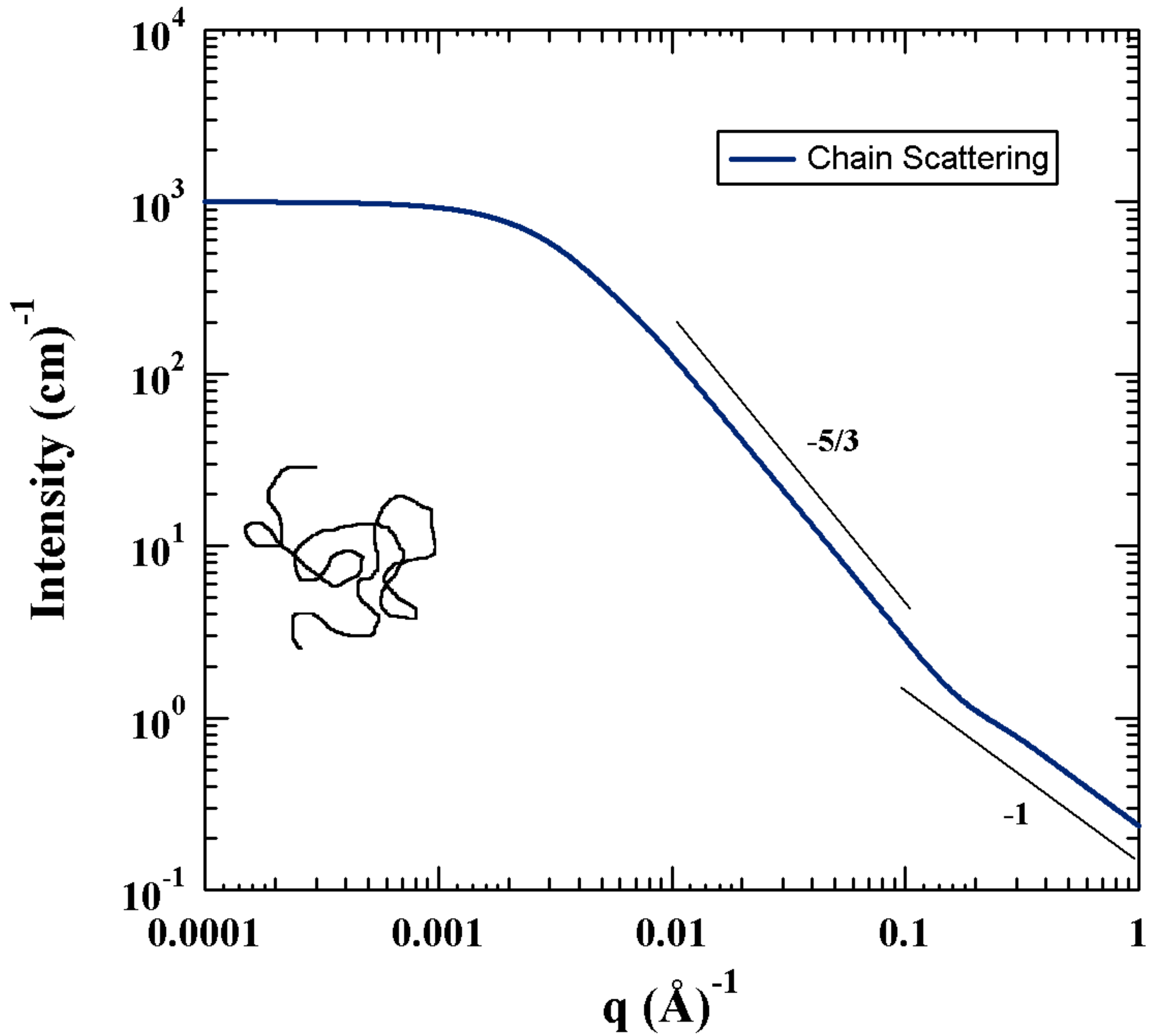

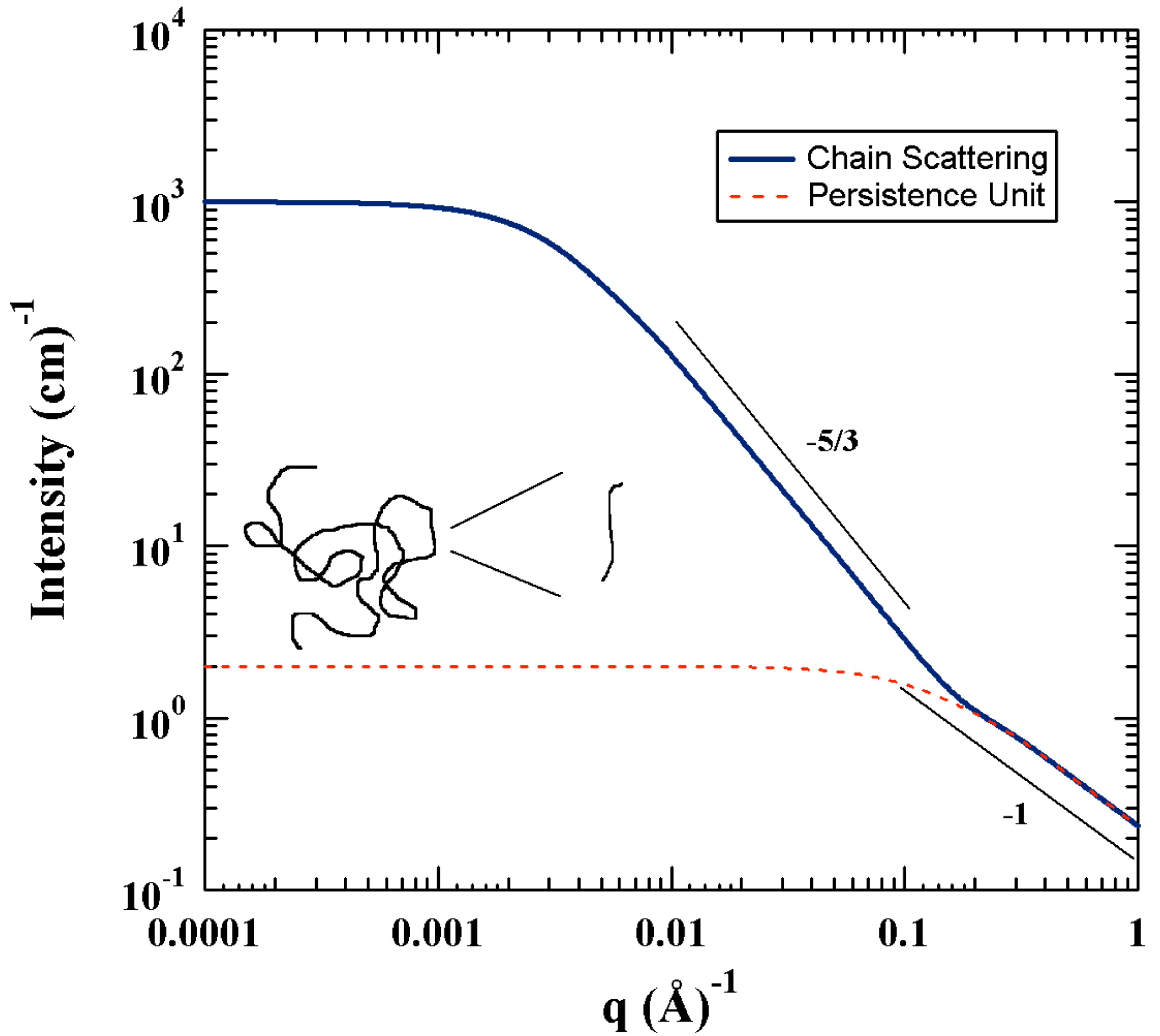

Persistence is distinct from chain scaling

Persistence Length of Short-Chain Branched Polyethylene Ramachandran R, Beaucage G, Kulkarni AS, McFaddin D, Merrick-Mack J, Galiatsatos V *Macromolecules* **41** 9802-9806 (2008).

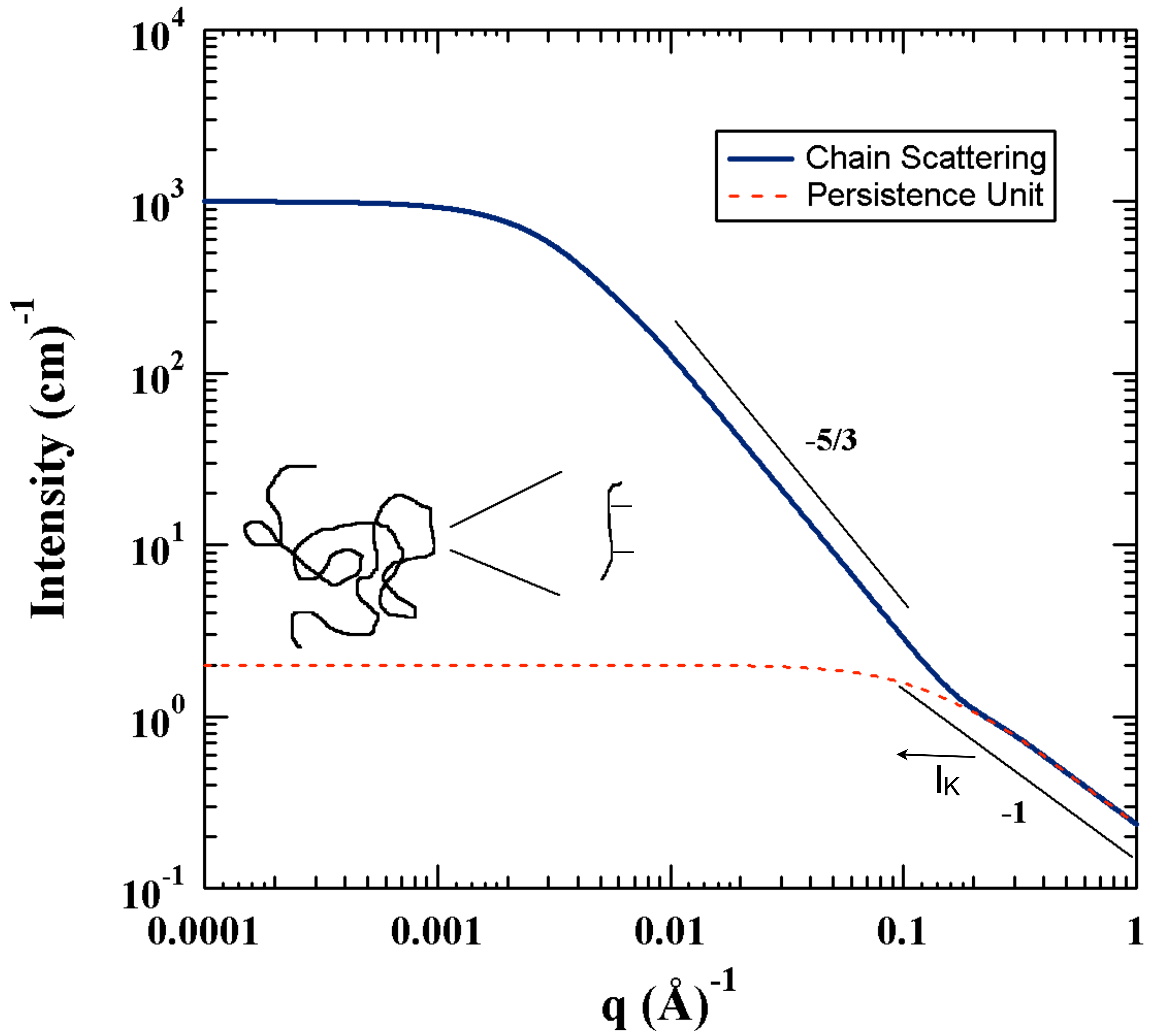

Persistence is distinct from chain scaling

Persistence Length of Short-Chain Branched Polyethylene Ramachandran R, Beaucage G, Kulkarni AS, McFaddin D, Merrick-Mack J, Galiatsatos V *Macromolecules* **41** 9802-9806 (2008).

Persistence Length vs. n_{SCB} for Polyethylene from SANS

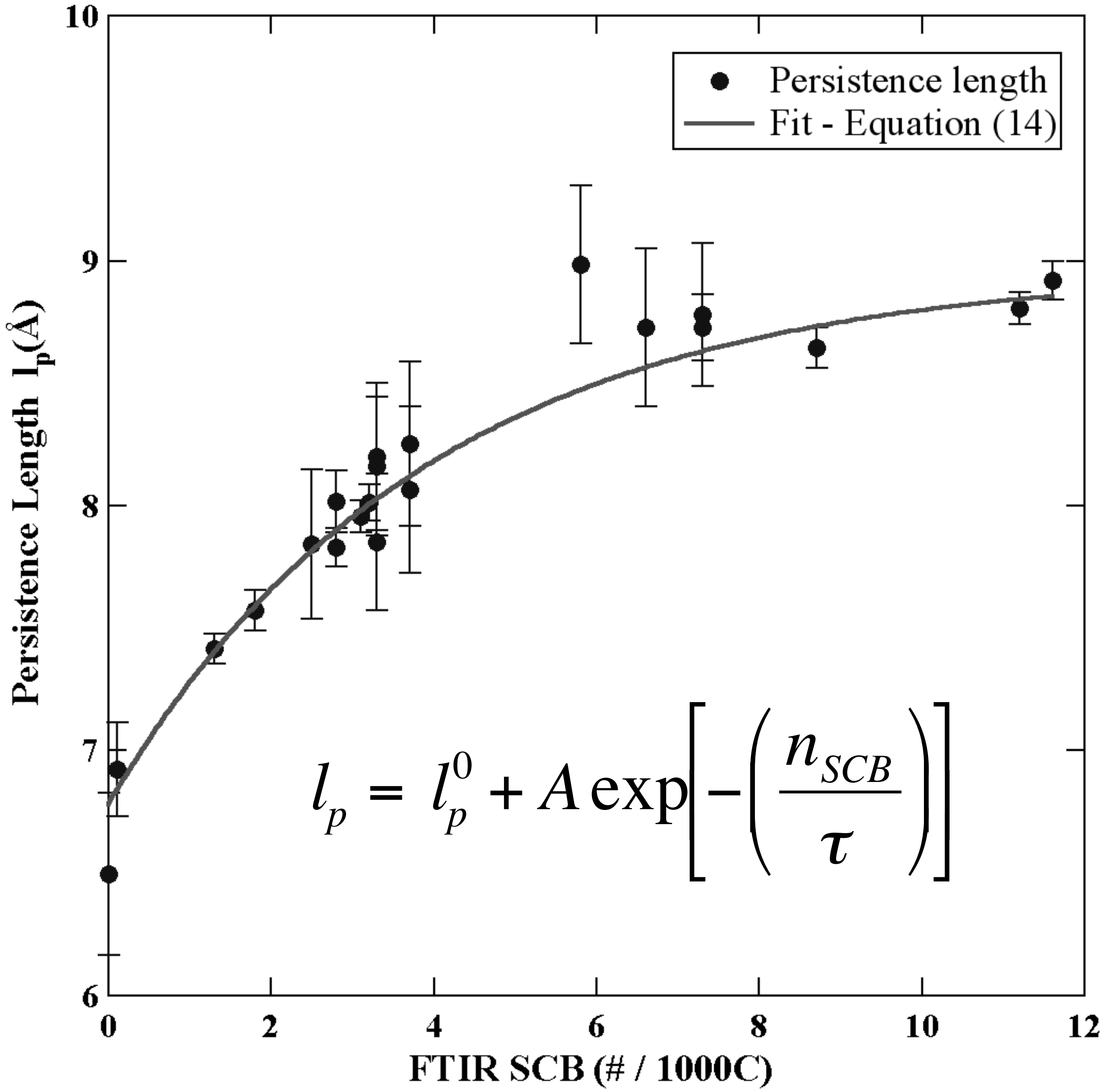

$l_p^0 = 8.9661 \pm 0.0788$ Å, $A = -2.1854 \pm 0.0989$, $\tau = 3.8949 \pm 0.519$

Limits: 6.78 Å and 8.97 Å

Persistence Length of Short-Chain Branched Polyethylene Ramachandran R, Beaucage G, Kulkarni AS, McFaddin D, Merrick-Mack J, Galiatsatos V *Macromolecules* **41** 9802-9806 (2008).

Fractal Hierarchical Structure
P = d_f

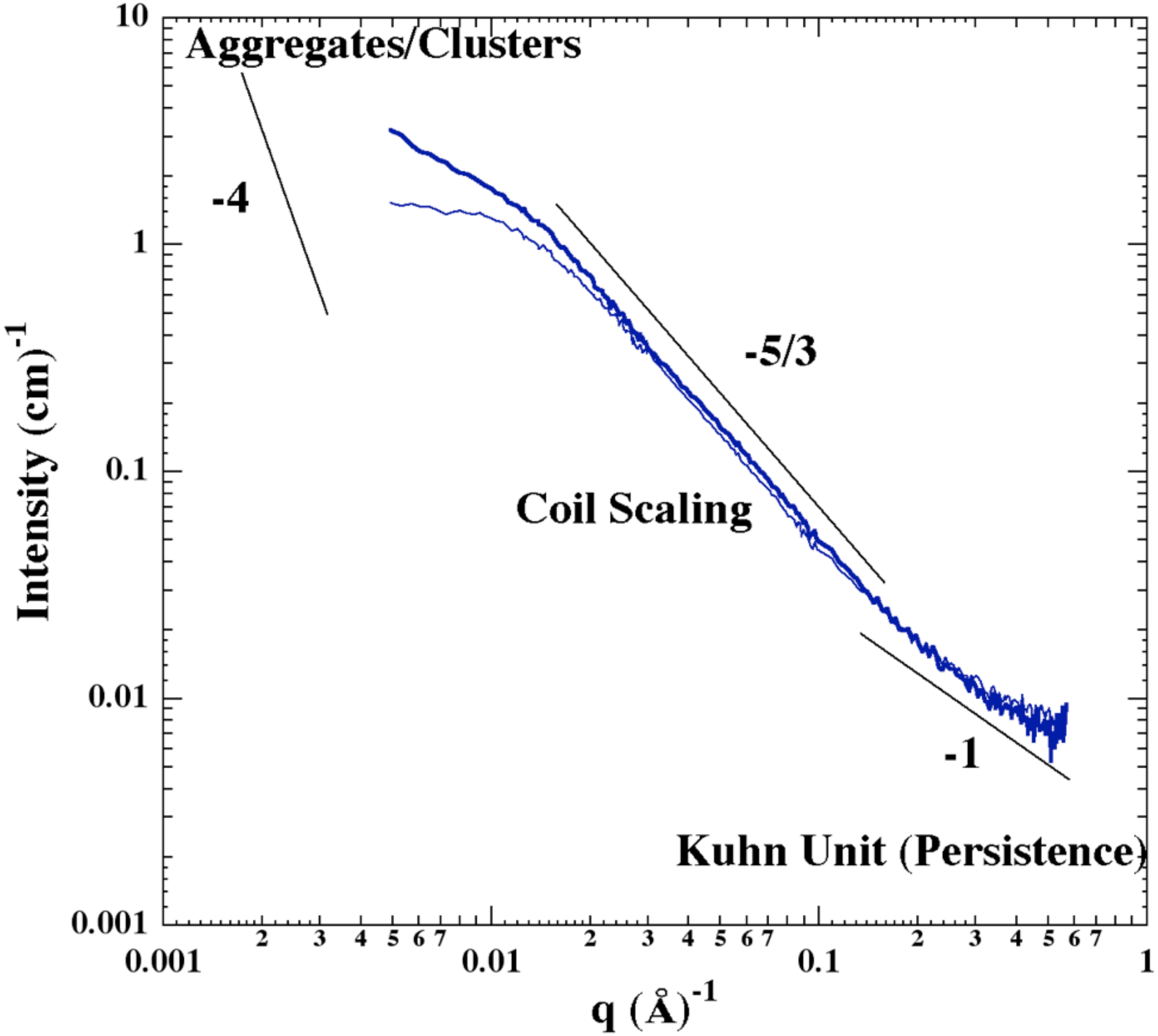

$I(q) \sim q^{df}$

Mass Fractal dimension, d_f

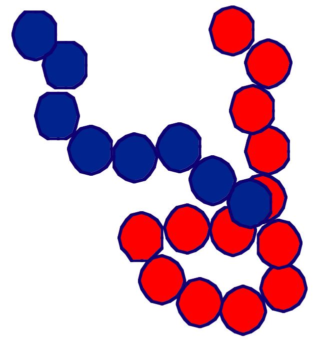

$$mass = z \sim \left(\frac{R}{d_p}\right)^{d_f}$$

z is mass/DOA
d_p is bead size
R is coil size

Random Aggregation (right) $d_f \sim 1.8$
Randomly Branched Gaussian $d_f \sim 2.3$
Self-Avoiding Walk $d_f = 5/3$

Problem:
  Disk $d_f = 2$
  Gaussian Walk $d_f = 2$

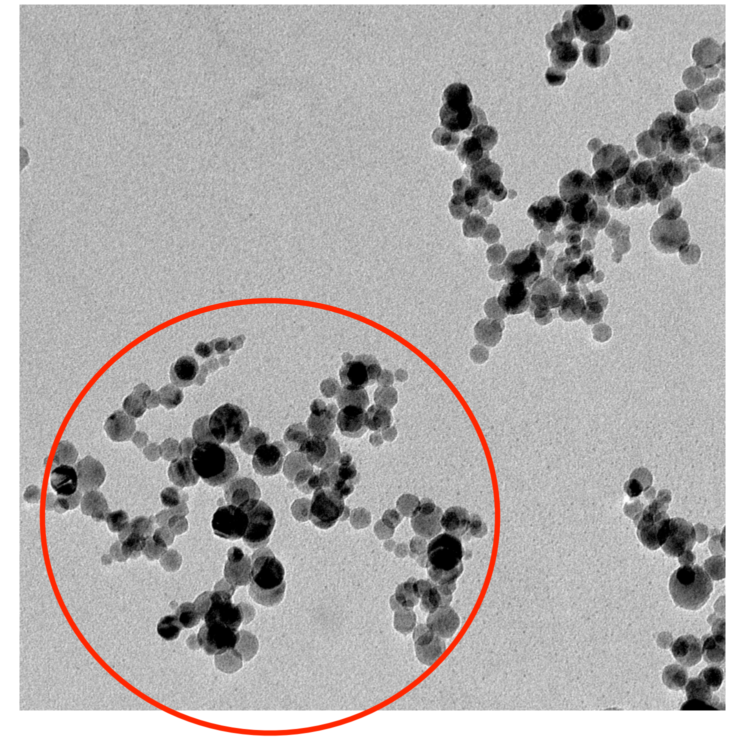

Nano-titania from Spray Flame

$R/d_p = 10$, $\alpha \sim 1$, $z \sim 220$
$d_f = \ln(220)/\ln(10) = 2.3$

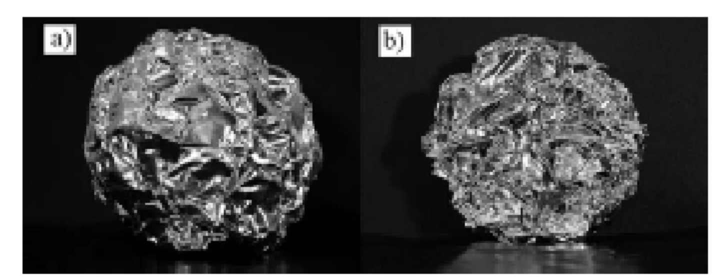

FIG. 1. Images of (a) balls folded from an aluminum sheet of thickness h=0.06 mm and edge size L=60 cm and (b) the cut through this ball. Balankin et al. (*Phys. Rev. E* **75** 051117

Mass Fractal dimension, d_f

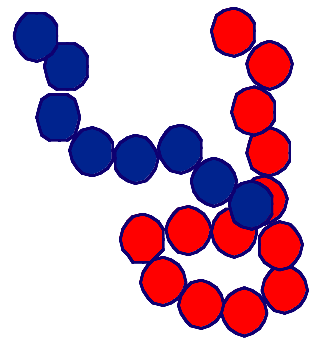

$$mass = z \sim \left(\frac{R}{d_p}\right)^{d_f}$$

z is mass/DOA
d_p is bead size
R is coil size

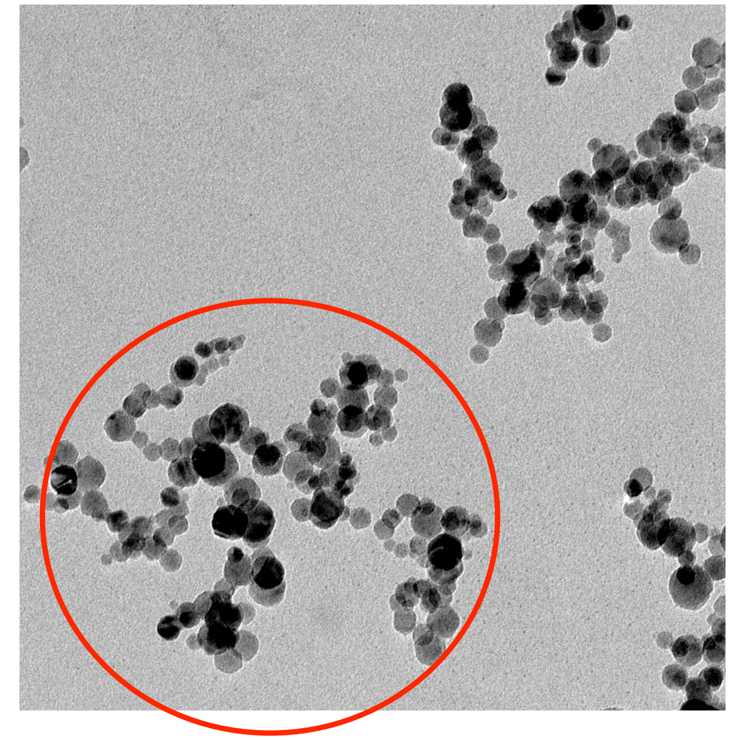

Nano-titania from Spray Flame

$R/d_p = 10$, $\alpha \sim 1$, $z \sim 220$
$d_f = \ln(220)/\ln(10) = 2.3$

Random Aggregation (right) $d_f \sim 1.8$
Randomly Branched Gaussian $d_f \sim 2.3$
Self-Avoiding Walk $d_f = 5/3$

Problem:
Disk $d_f = 2$
Gaussian Walk $d_f = 2$

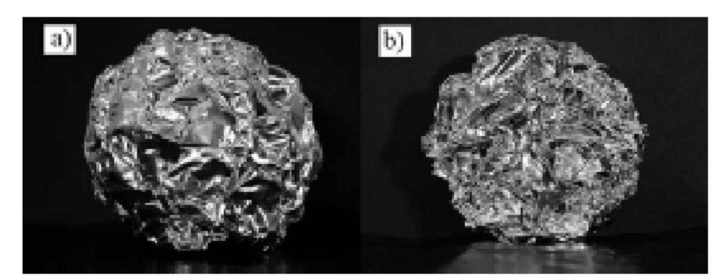

FIG. 1. Images of (a) balls folded from an aluminum sheet of thickness h=0.06 mm and edge size L=60 cm and (b) the cut through this ball. Balankin et al. (*Phys. Rev. E* **75** 051117

A measure of topology is not given by d_f.
Disk and coil are topologically different.
Foil and disk are topologically similar.

Complex Structures Can be Decomposed

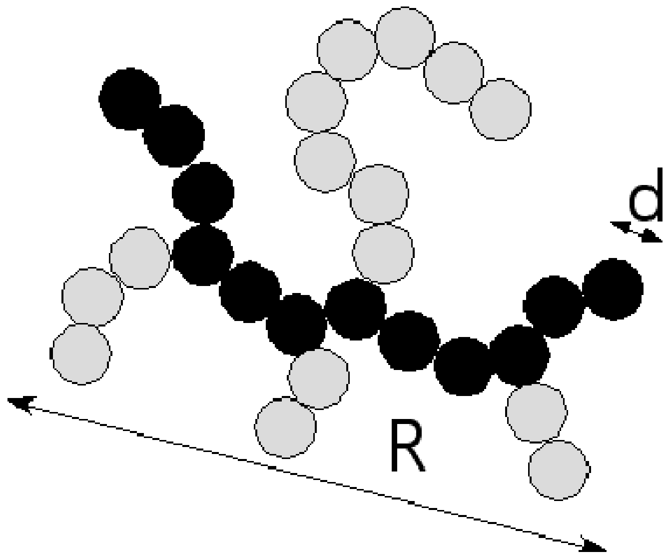

Tortuosity

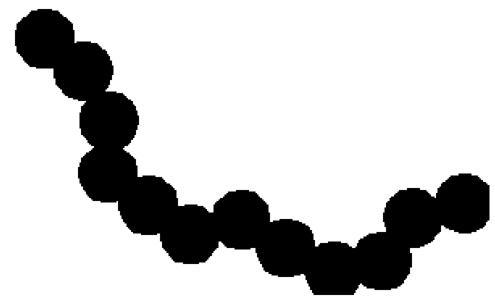

Connectivity

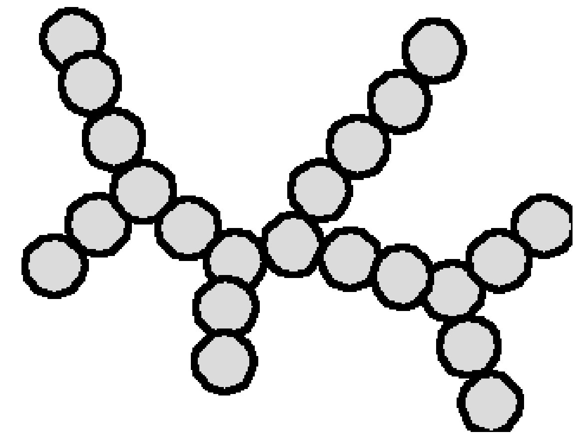

$$z \sim \left(\frac{R}{d}\right)^{d_f} \sim p^c \sim s^{d_{\min}}$$

$$p \sim \left(\frac{R}{d}\right)^{d_{\min}}$$

$$s \sim \left(\frac{R}{d}\right)^{c}$$

$$d_f = d_{\min} c$$

z	d_f	p	d_{min}	s	c	R/d
27	1.36	12	1.03	22	1.28	11.2

Complex Structures Can be Decomposed

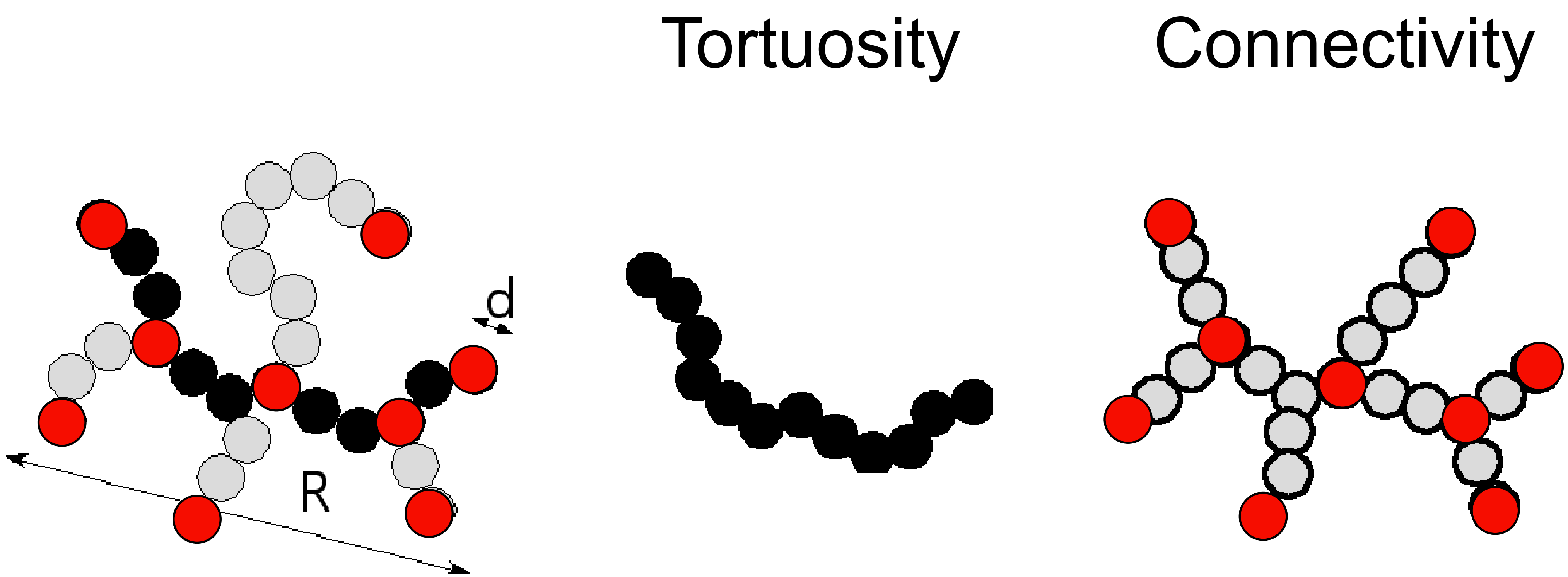

$$z \sim \left(\frac{R}{d}\right)^{d_f} \sim p^c \sim s^{d_{min}}$$

$$p \sim \left(\frac{R}{d}\right)^{d_{min}}$$

$$s \sim \left(\frac{R}{d}\right)^{c}$$

$$d_f = d_{min} c$$

z	d_f	p	d_{min}	s	c	R/d
27	1.36	12	1.03	22	1.28	11.2

Beaucage G, *Determination of branch fraction and minimum dimension of fractal aggregates* Phys. Rev. E **70** 031401 (2004).

Complex Structures Can be Decomposed

Tortuosity | Connectivity

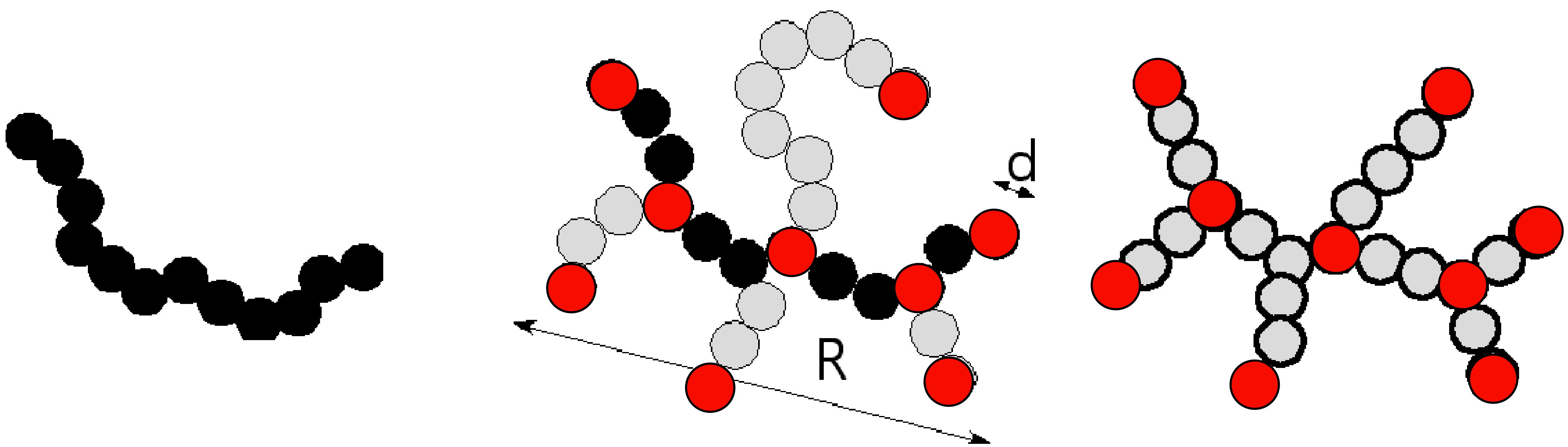

$$\phi_{Br} = \frac{z - p}{z} = 1 - z^{1/c - 1}$$

0.56

$$\phi_M = \frac{z - s}{z} = 1 - z^{1/d_{min} - 1}$$

0.19

z	d_f	p	d_{min}	s	c	R/d
27	1.36	12	1.03	22	1.28	11.2

Beaucage G, *Determination of branch fraction and minimum dimension of fractal aggregates* Phys. Rev. E **70** 031401 (2004).

Consider a Crumpled Sheet

A 2-d Sheet has c = 2
d_{min} depends on the extent of crumpling

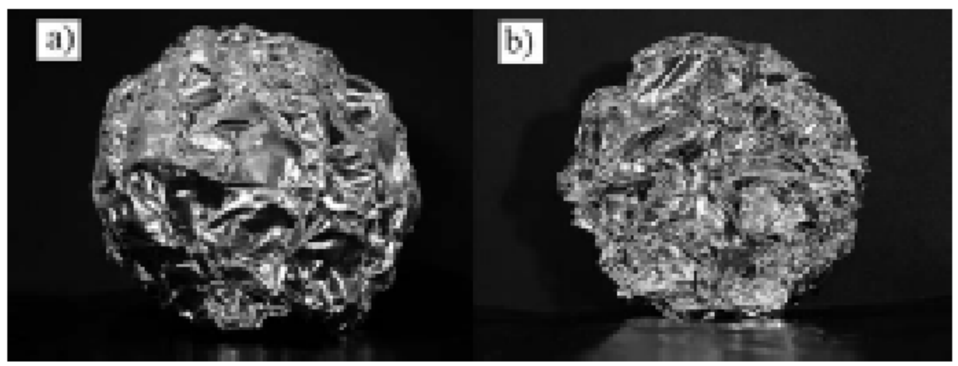

FIG. 1. Images of (a) balls folded from an aluminum sheet of thickness h=0.06 mm and edge size L=60 cm and (b) the cut through this ball.

$$d_f = 2.3$$
$$d_{\min} = 1.15$$
$$c = 2$$

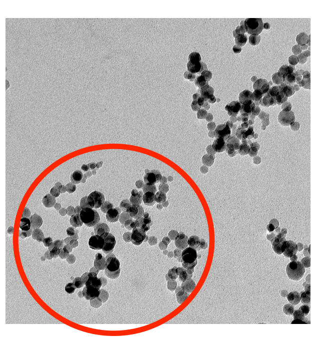

$$d_f = 2.3$$
$$d_{\min} = 1.47$$
$$c = 1.56$$

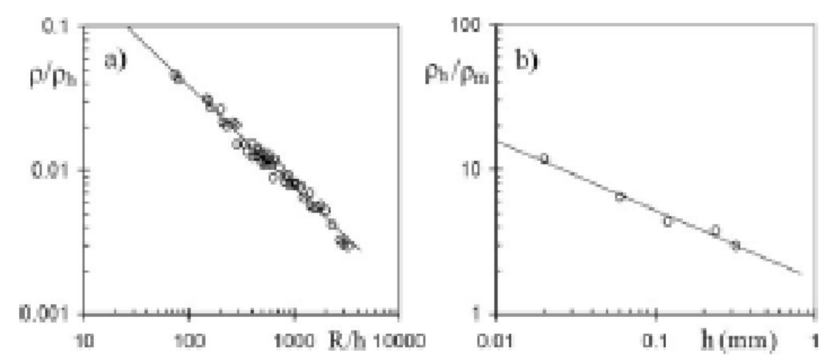

FIG. 3. (a) Data collapse for ρ/ρ_h versus R/h (the slope of the fitting line is $3-D=0.7009$, $R^2=0.98$); and (b) log-log plot of ρ_h/ρ_m versus h (straight line is given by $y=1.728x^{-0.4816}$, $R^2=0.98$).

Balankin et al. (*Phys. Rev. E* **75** 051117 (2007))

Disk

$$d_f = 2$$

$$d_{\min} = 1$$

$$c = 2$$

Extended β-sheet (misfolded protein)

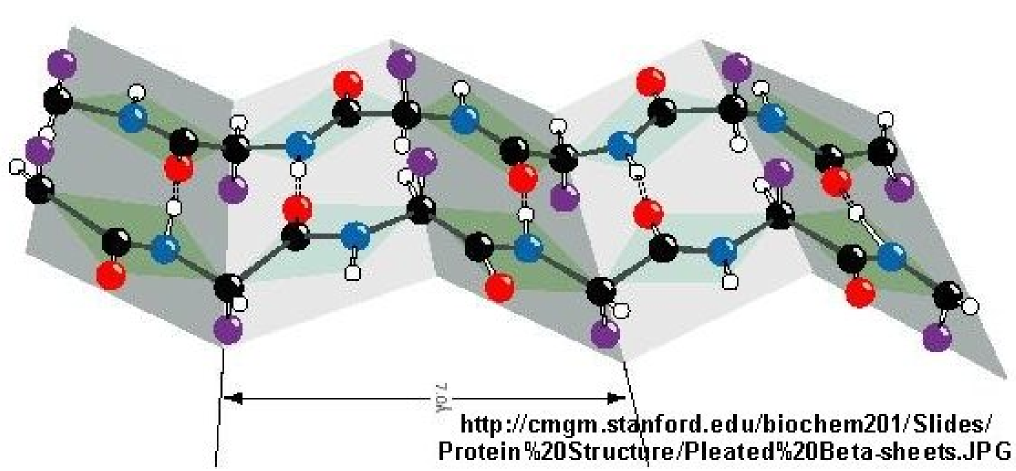

Random Coil

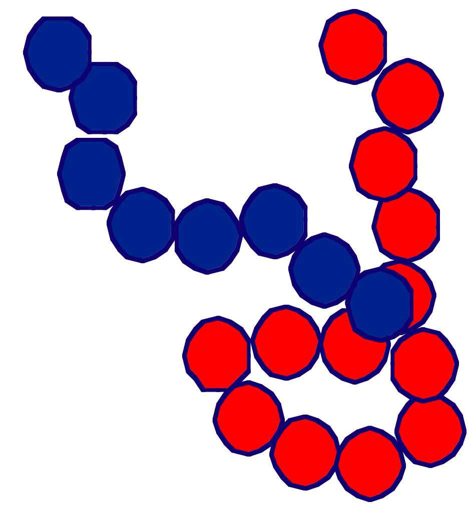

$$d_f = 2$$

$$d_{\min} = 2$$

$$c = 1$$

Unfolded Gaussian chain

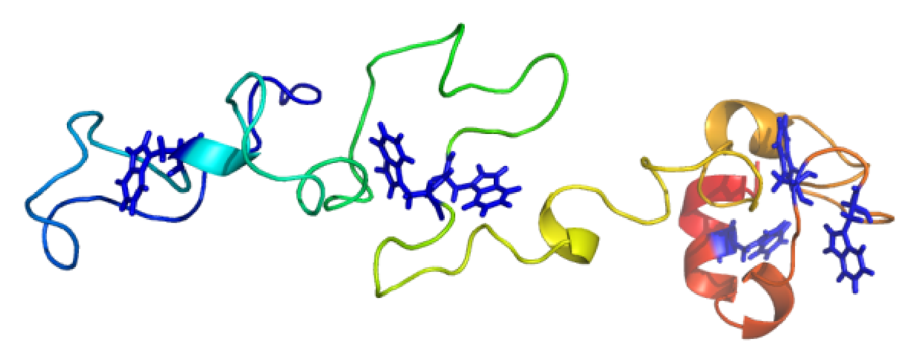

We have resolved a complex structure into a *topological network* of branch sites and a *tortuous path* through the structure

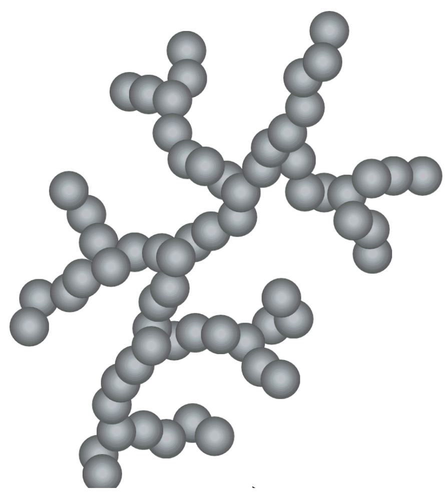

z, d_f

Topological Network

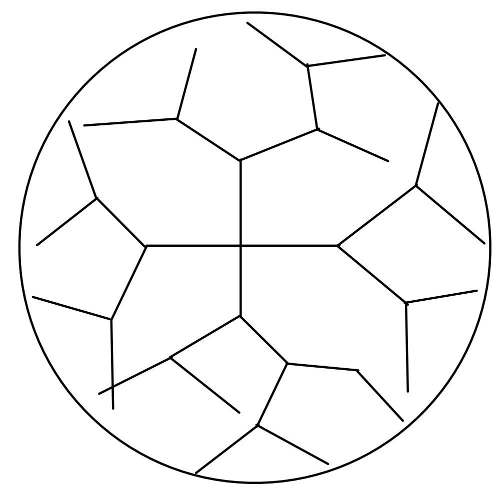

s, c

Tortuous Path

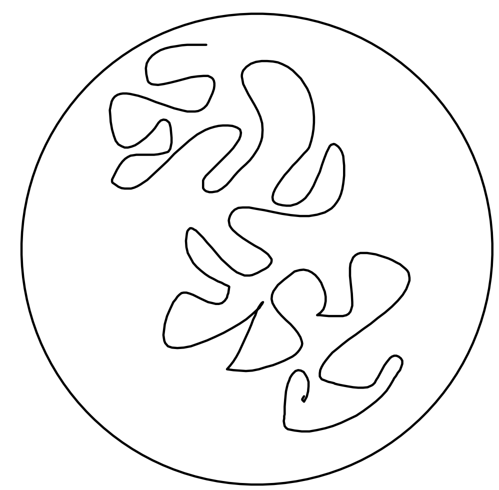

p, d_{min}

Polymers *Synthesis* *Thermodynamics*

Mechanics *Drag Coefficient* *Spring Constant*

Many other interpretations: Consider a sheet of paper and a crumpled sheet.

Neutron & X-ray Scattering

We can "Build" a Scattering Pattern from Structural Components using Some Simple Scattering Laws

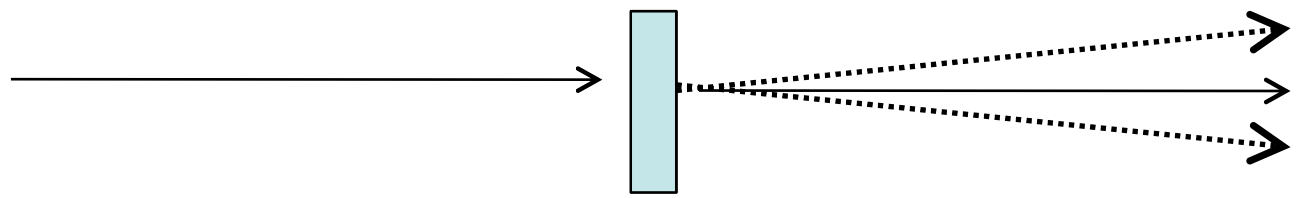

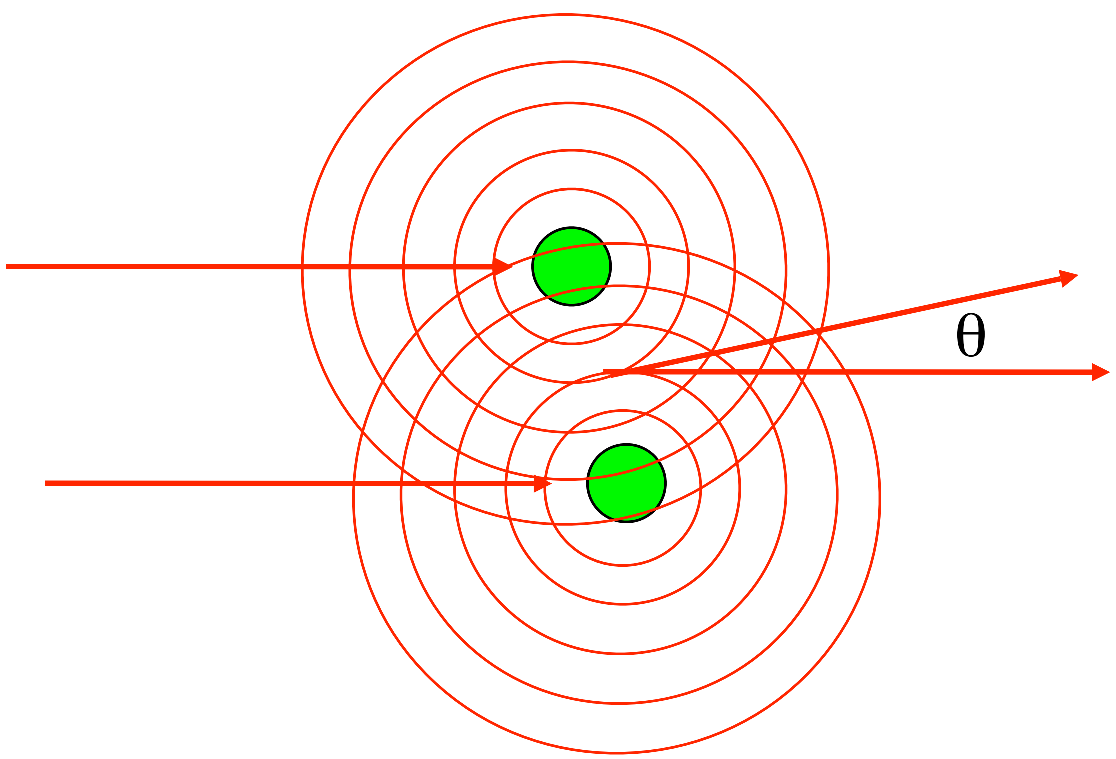

I(θ) is related to amount Nn^2

θ is related to size/distances

$$q = \frac{4\pi}{\lambda}\sin\left(\theta/2\right)$$

$$d = \frac{2\pi}{q}$$

-Dilute Solution of Polymer
-Use Deuterated Solvent to Enhance Contrast (for SANS)
-40 minutes Measurement using 2 mg of Hydrogeneous Sample

Small-Angle Scattering for Mass Fractals of Variable Topology

$d_f = 2$
$c = 2$
$d_{min} = 1$

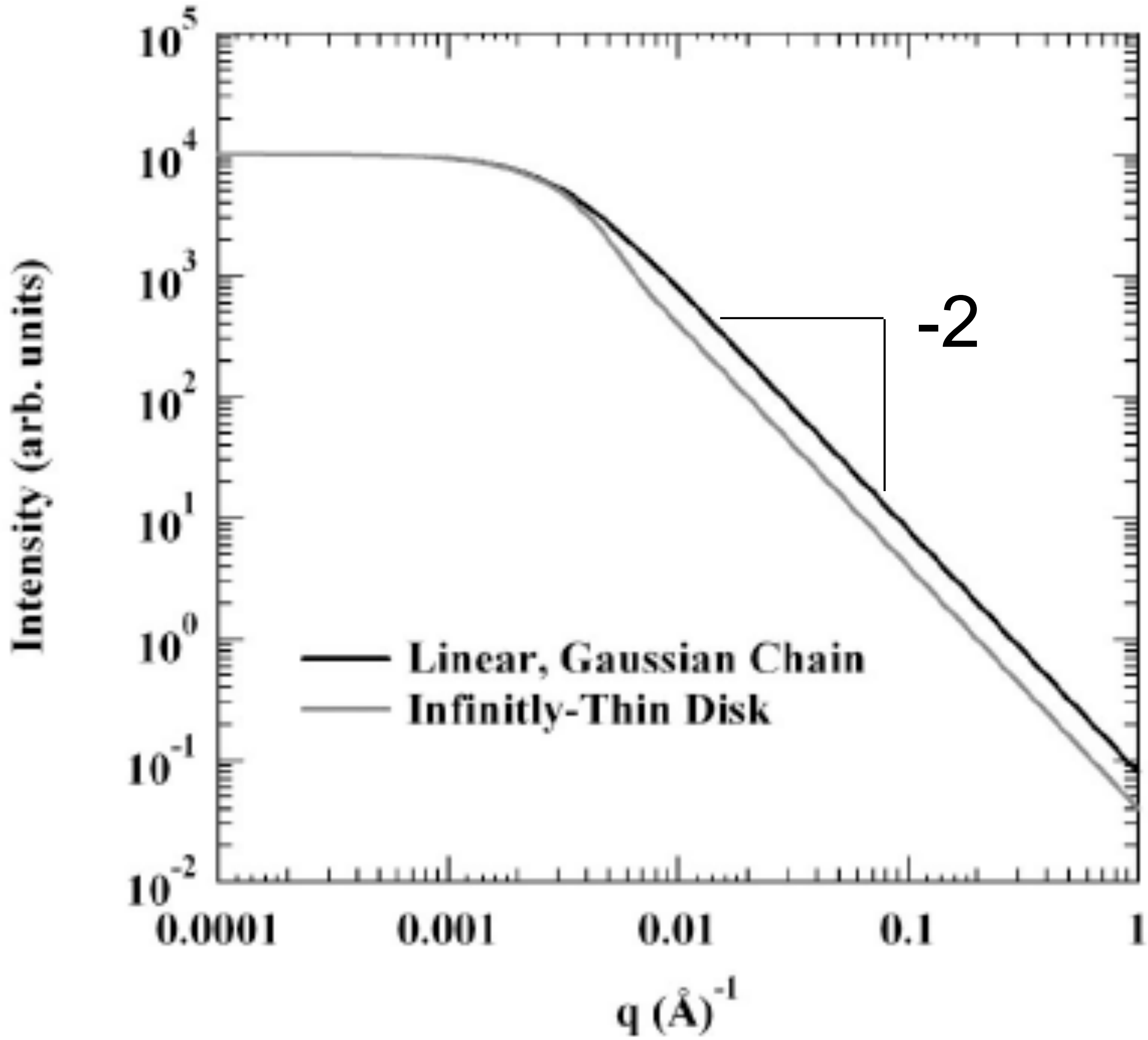

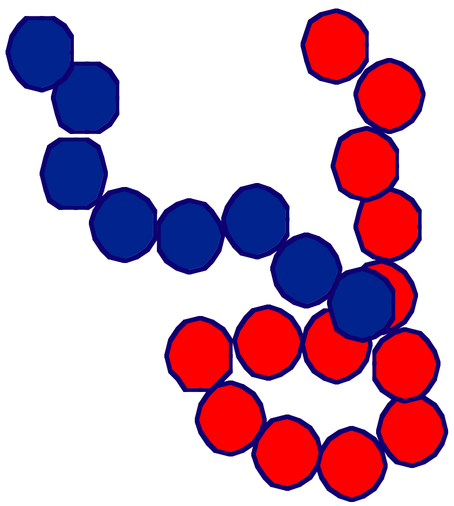

$d_f = 2$
$c = 1$
$d_{min} = 2$

Beaucage G, *Determination of branch fraction and minimum dimension of fractal aggregates* Phys. Rev. E **70** 031401 (2004).

Guinier's Law

$$I(q) = G e^{\frac{-q^2 R_g^2}{3}}$$

G, R_g

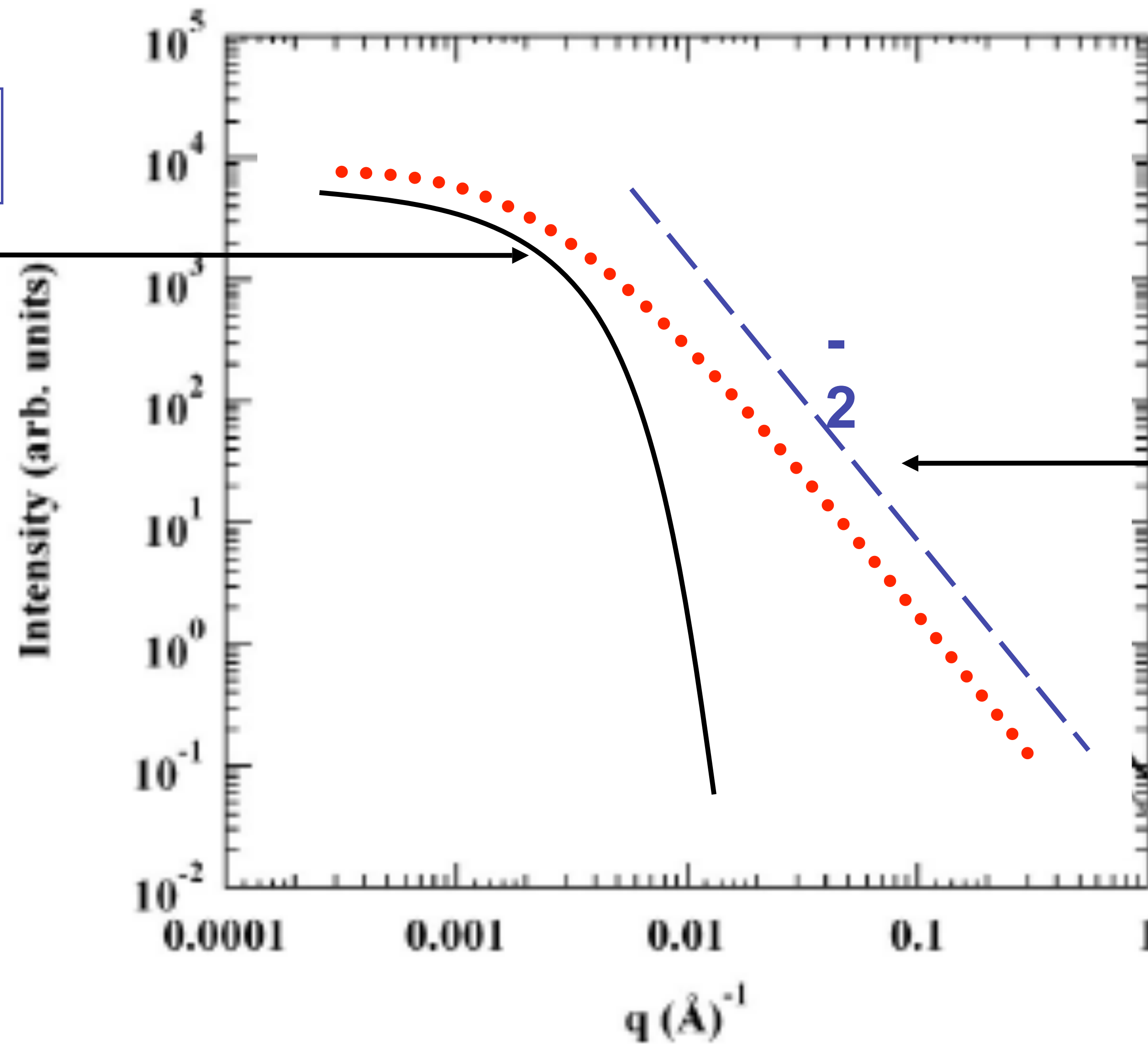

Power Law

$$I(q) = B_f\, q^{-d_f}$$

B_f, d_f

Thin Disk

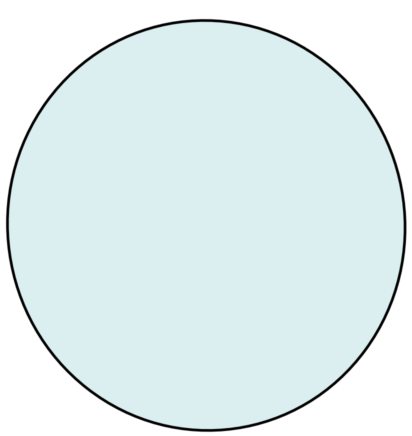

$$d_{\min} = \frac{B_f R_{g,2}^{d_f}}{G_2 \Gamma\left(d_f / 2\right)}$$

Gaussian Chain

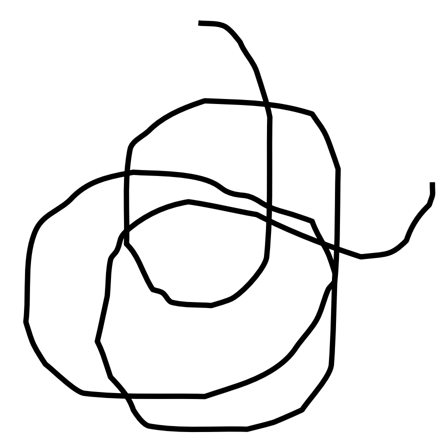

Beaucage G, *Determination of branch fraction and minimum dimension of fractal aggregates* Phys. Rev. E **70** 031401 (2004).

Guinier's Law

$$I(q) = G e^{\frac{-q^2 R_g^2}{3}}$$

G, R_g

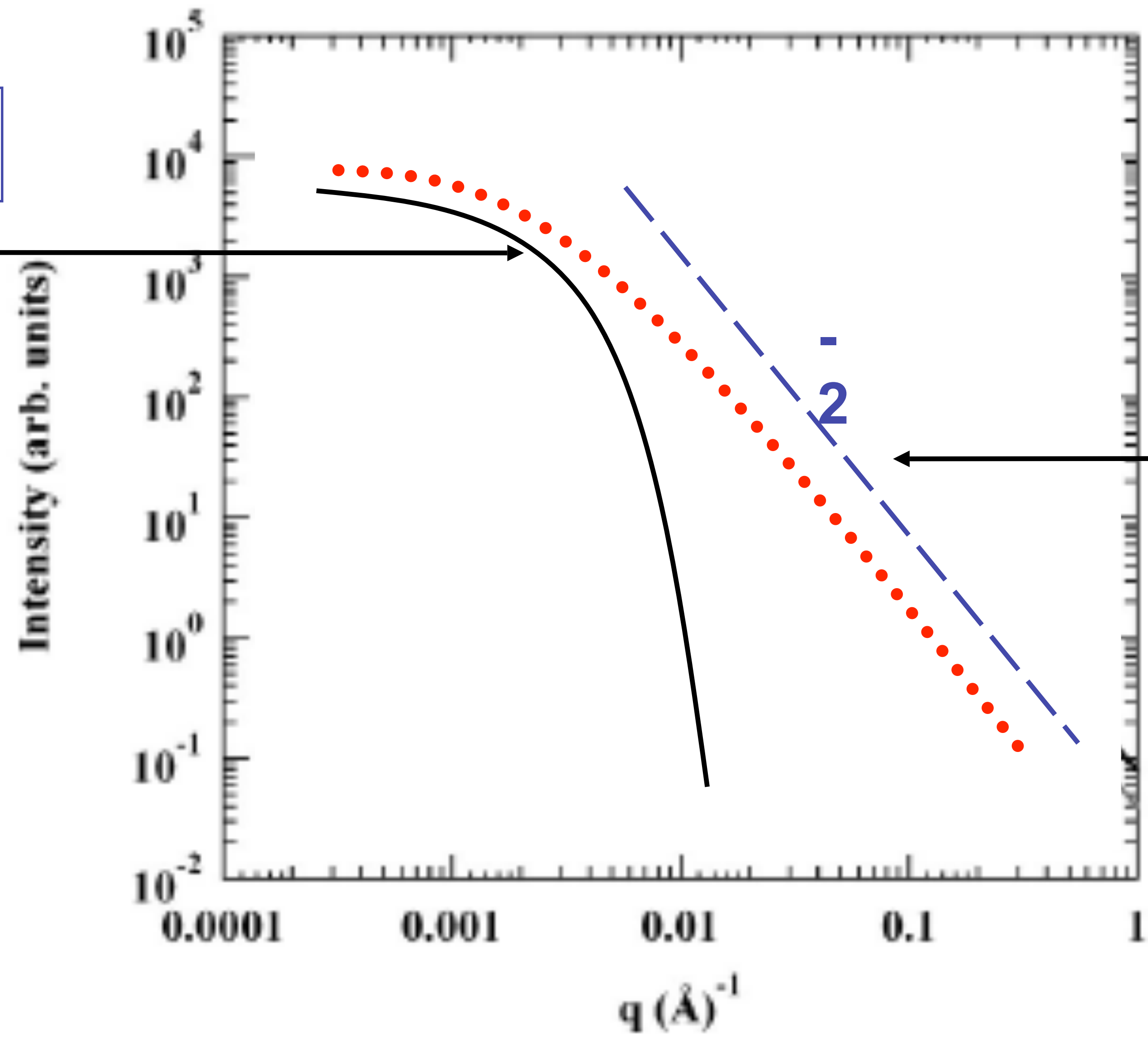

Power Law

$$I(q) = B_f \, q^{-d_f}$$

B_f, d_f

Measure d_{min}, d_f and know or measure z:

$$c = \frac{d_f}{d_{min}} \qquad p = z^{1/c} \qquad s = z^{1/d_{min}}$$

$$\phi_{Br} = \frac{z - p}{z} = 1 - z^{1/c - 1} \qquad \phi_M = \frac{z - s}{z} = 1 - z^{1/d_{min} - 1}$$

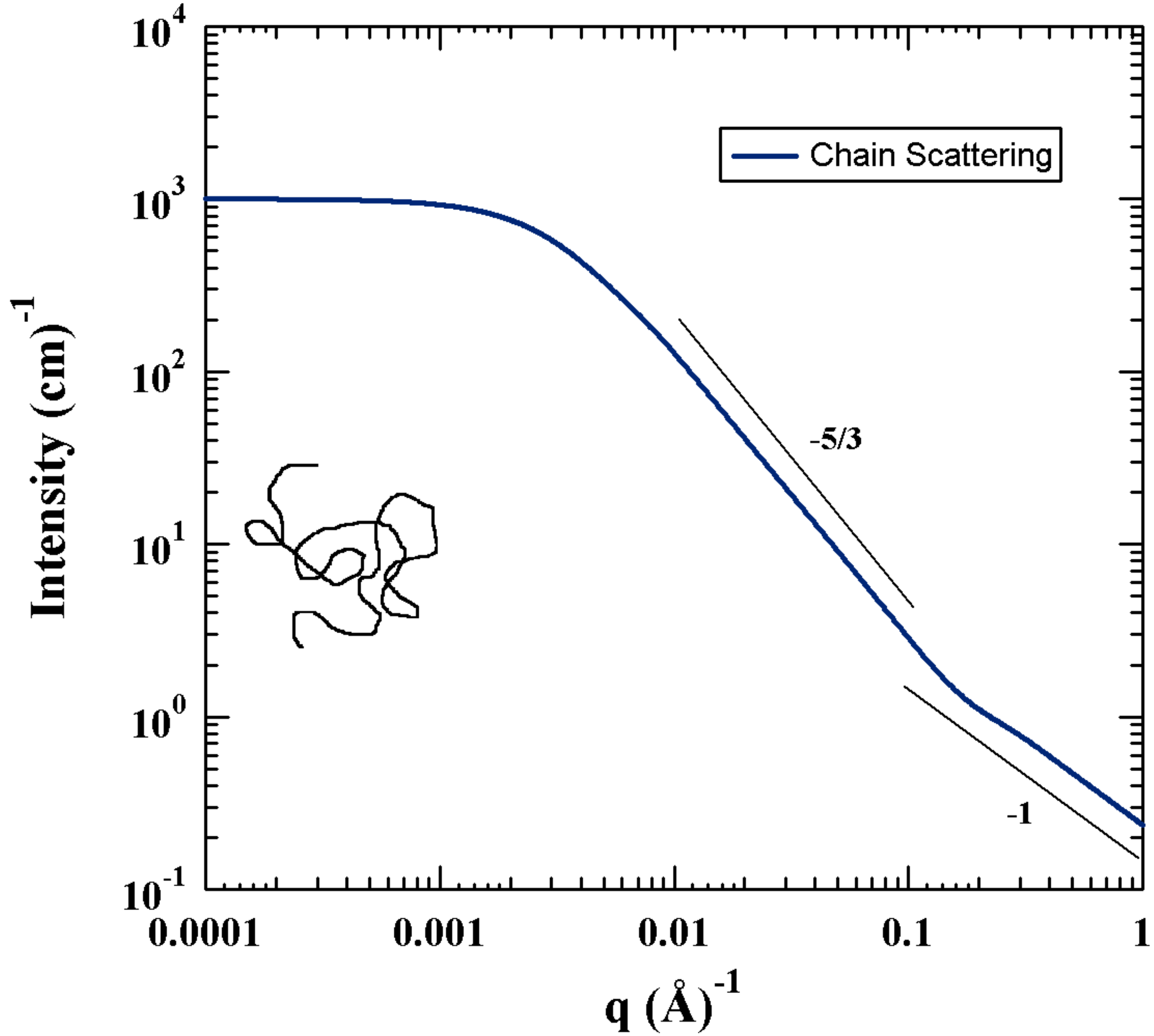
Chain Scattering
-5/3
-1
Intensity (cm)-1
q (Å)-1
10-1
100
101
102
103
104
0.0001
0.001
0.01
0.1
1

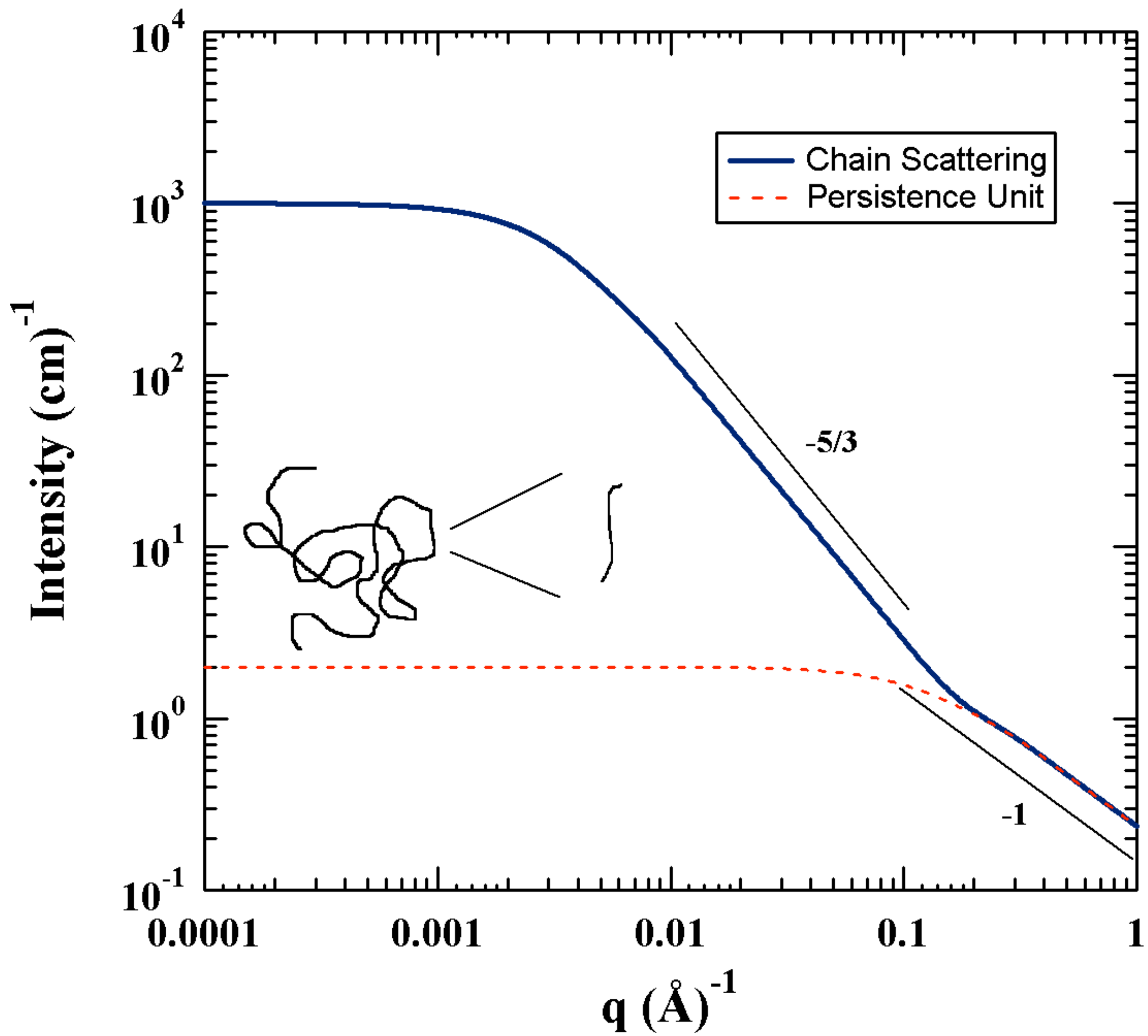

Persistence is distinct from chain scaling

Persistence Length of Short-Chain Branched Polyethylene Ramachandran R, Beaucage G, Kulkarni AS, McFaddin D, Merrick-Mack J, Galiatsatos V *Macromolecules* **41** 9802-9806 (2008).

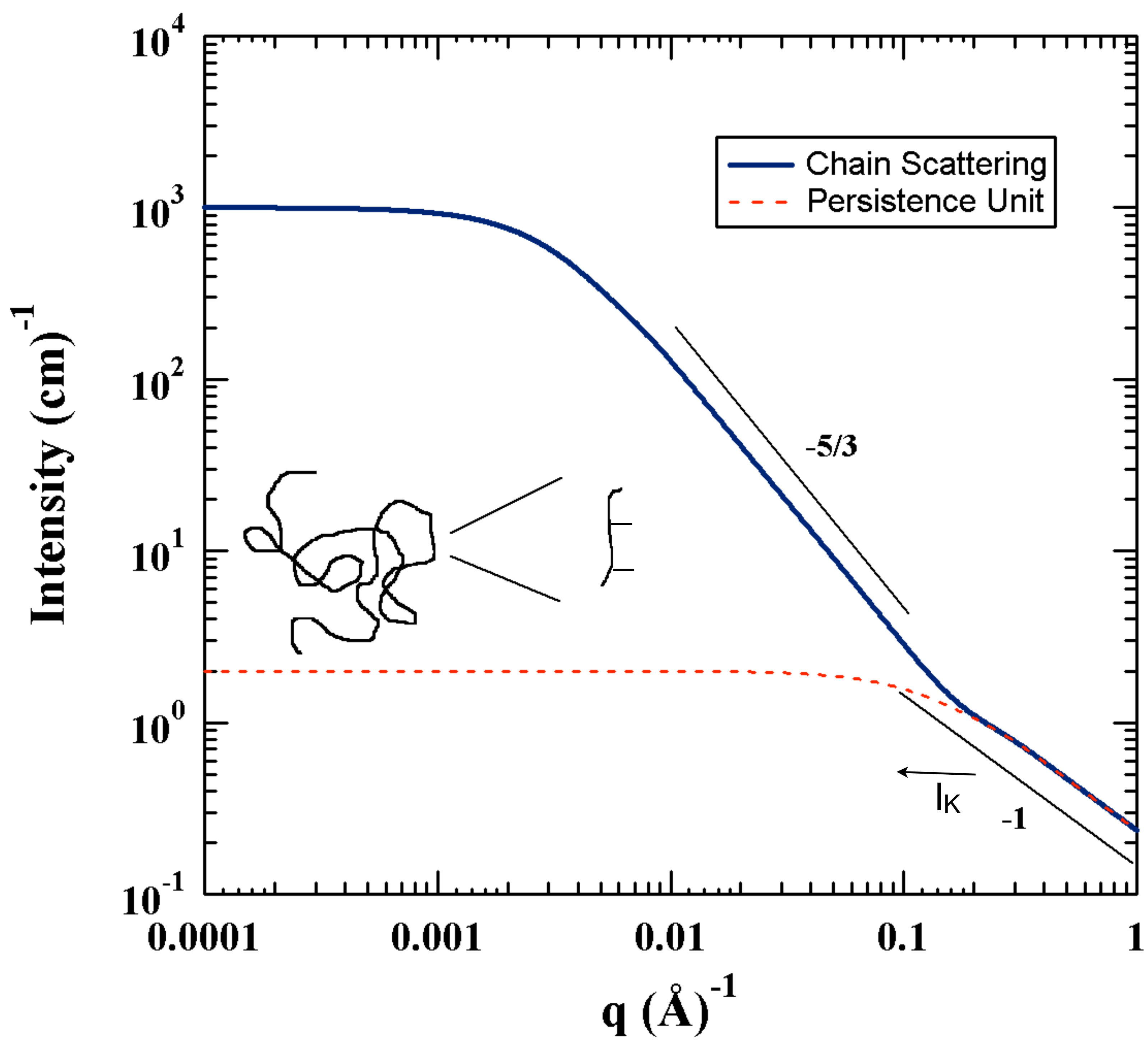

Persistence is distinct from chain scaling

Persistence Length of Short-Chain Branched Polyethylene Ramachandran R, Beaucage G, Kulkarni AS, McFaddin D, Merrick-Mack J, Galiatsatos V *Macromolecules* **41** 9802-9806 (2008).

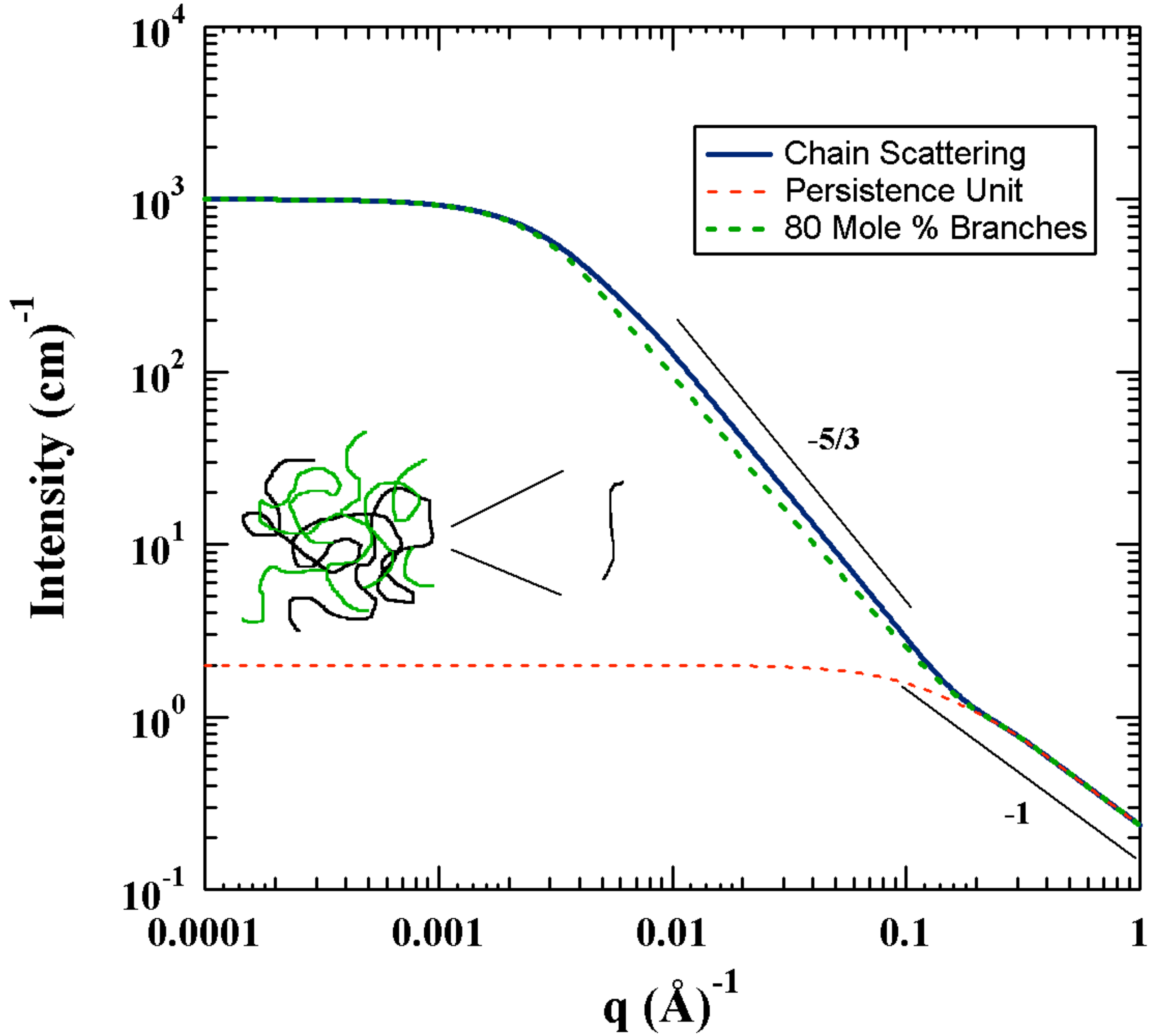

Branching has a quantifiable signature.

Branch content of metallocene polyethylene Ramachandran R, Beaucage G, Kulkarni AS, McFaddin D, Merrick-Mack J, Galiatsatos V *Macromolecules*, **42** 4746-4750 (2009).

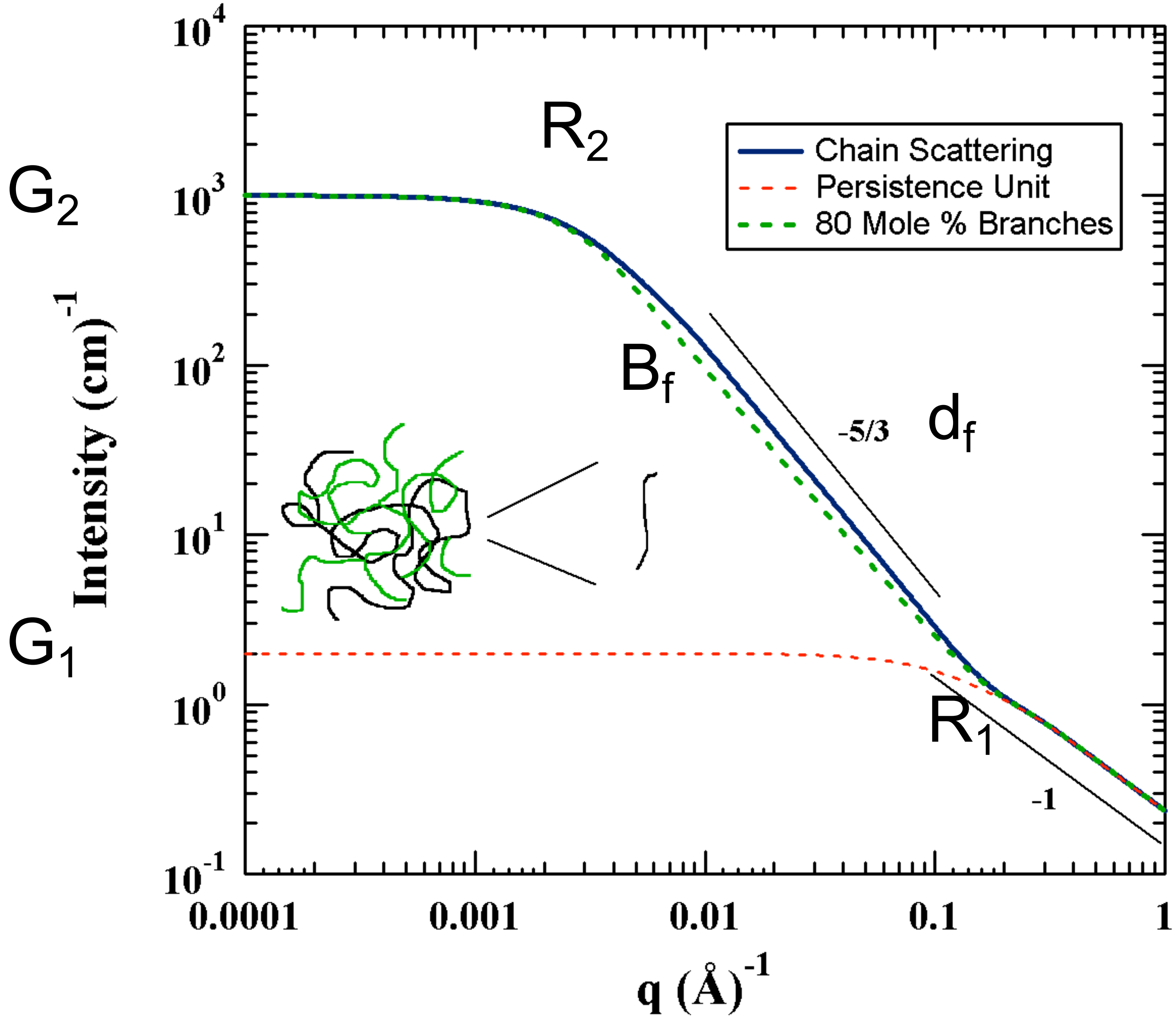

G2
G1
R2
Bf
df
R1
-5/3
-1
Chain Scattering
Persistence Unit
80 Mole % Branches
Intensity (cm)-1
q (Å)-1
0.0001
0.001
0.01
0.1
1

$$d_{min} = \frac{B_f R_{g,2}^{d_f}}{G_2 \Gamma\left(d_f/2\right)}$$

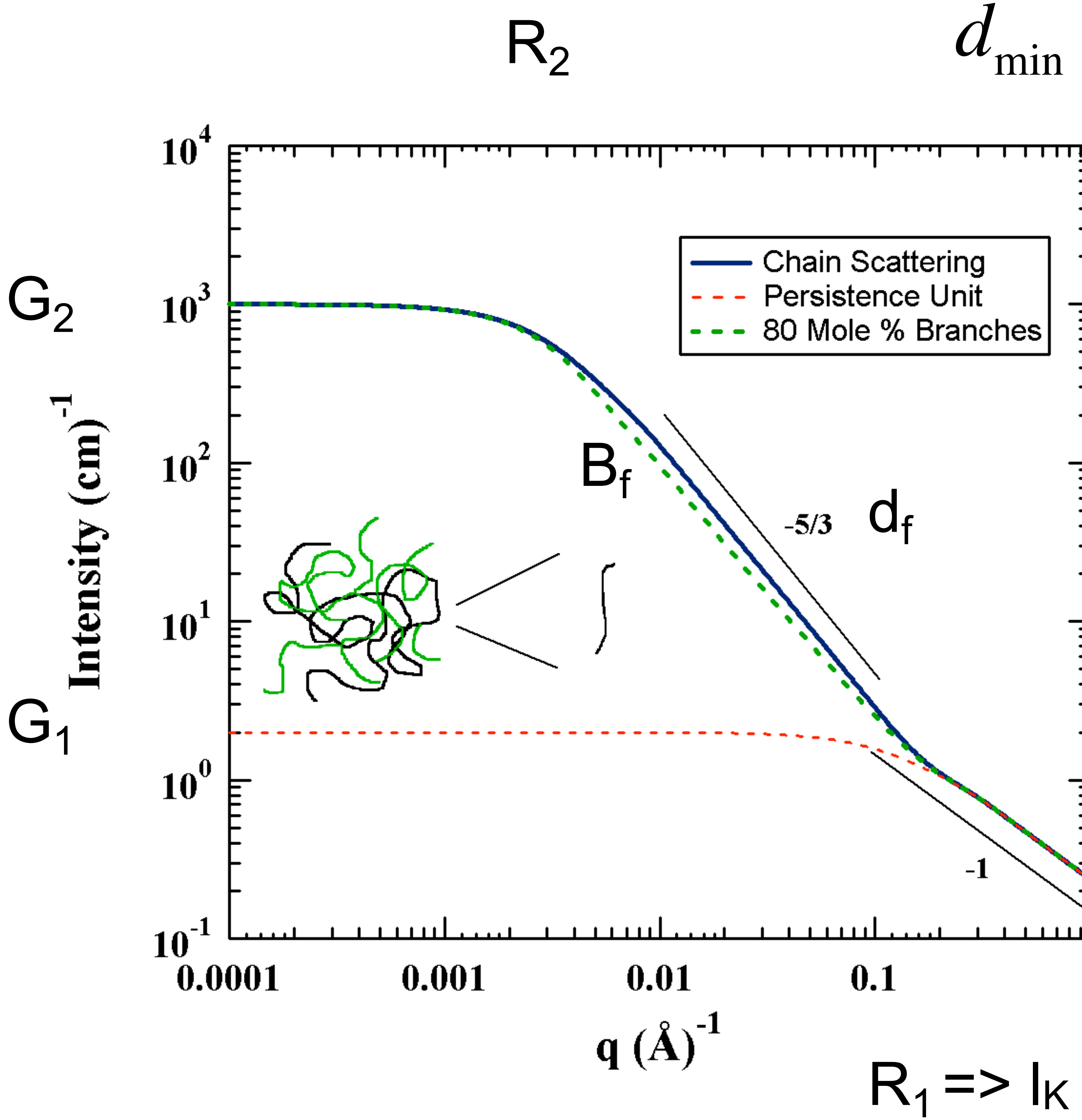

Beaucage G, *Determination of branch fraction and minimum dimension of fractal aggregates* Phys. Rev. E **70** 031401 (2004).

Branching dimensions are obtained by combining local scattering laws

Quantification of Branching

$$c = \frac{d_f}{d_{\min}} \qquad p = z^{1/c} \qquad s = z^{1/d_{\min}}$$

$$\phi_{Br} = \frac{z - p}{z} = 1 - z^{1/c-1}$$

$$z_{Br} = \frac{z\phi_{Br}}{n_{Br,NMR \text{ or } IR}}$$

n_{Br} from SANS (in Good Solvent)

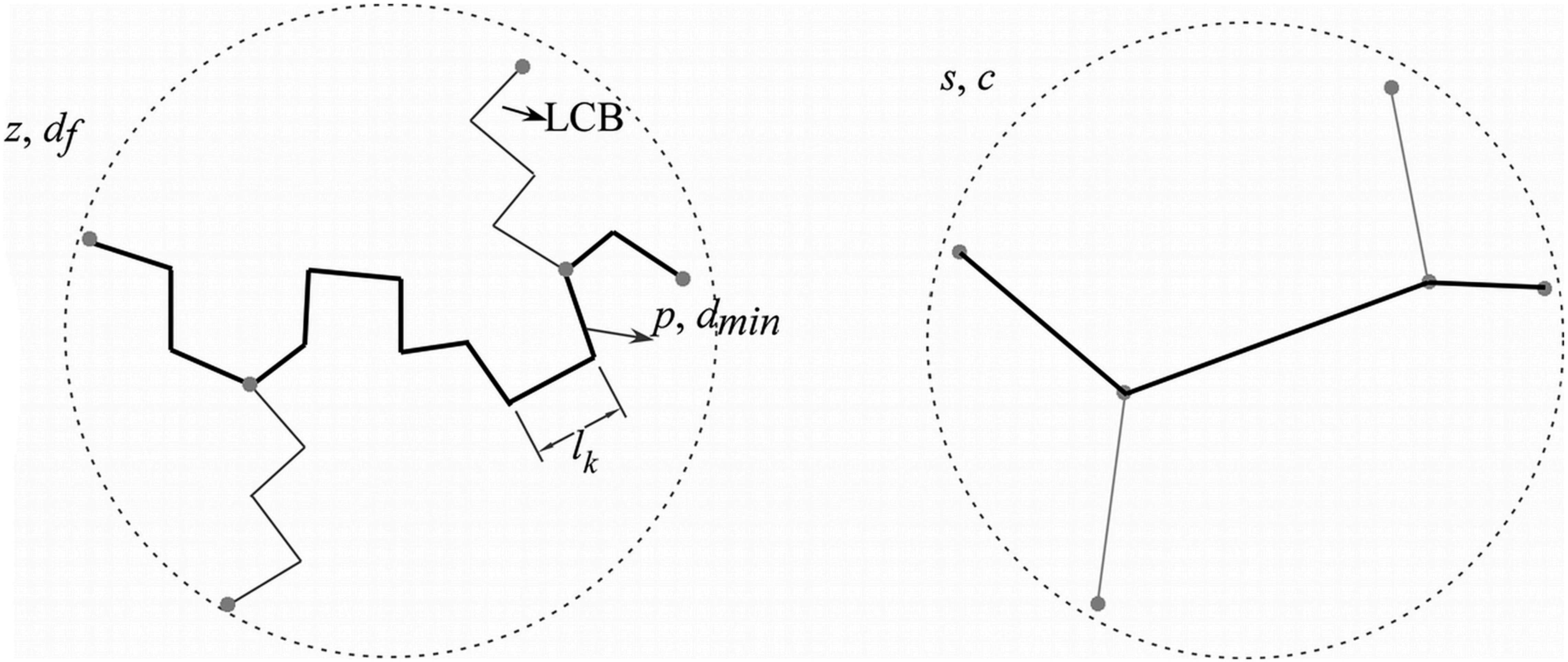

$$r = n_{s,p}\left(\frac{p}{n_{s,p}}\right)^{3/5}$$

$$r = p^{1/d_{min}}$$

$$n_{s,p} = \left[p^{(1/d_{min})-(3/5)}\right]^{5/2}$$

$$n_{br,p} = n_{s,p} - 1$$

$$n_{k,s} = \frac{p}{n_{br,p}+1} = \frac{z}{2n_{br}+1}$$

$$n_{br} = \frac{z^{[(5/2d_f)-(3/2c)]+[1-(1/c)]}-1}{2}$$

$$z_{br} = \frac{z\phi_{br}M_{Kuhn}}{n_{br}}$$

Branch content of metallocene polyethylene Ramachandran R, Beaucage G, Kulkarni AS, McFaddin D, Merrick-Mack J, Galiatsatos V *Macromolecules*, **42** 4746-4750 (2009).

Dow HDB Series
Metallocene-Catalyzed Model Branched PE Chains
(Courtesy L. J. Effler and A. W. deGroot)

Table 1. Characterization of Long-Chain Branching in Dow HDB Samples

sample	LCB/10^3C ^{13}C NMR[a]	M_n (g/mol)[a]	PDI (M_w/M_n)[a]	β	n_{br}	$n_{br,p}$	ϕ_{br}	z_{br} (g/mol)
HDB-1	0.026	39 300	1.98	0.073	0.080 ± 0.004	0.047 ± 0.005	0.10 ± 0.02	12 700 ± 1500
HDB-2	0.037	41 500	1.93	0.110	0.115 ± 0.005	0.053 ± 0.005	0.14 ± 0.02	17 400 ± 1600
HDB-3	0.042	41 200	1.99	0.124	0.144 ± 0.007	0.065 ± 0.005	0.17 ± 0.02	16 500 ± 1600
HDB-4	0.080	39 200	2.14	0.224	0.262 ± 0.007	0.090 ± 0.008	0.28 ± 0.03	18 600 ± 1700

Table 2. Size and Dimensions of Dow HDB Samples Measured from SANS

sample	R_g (Å)	d_f	c	l_p (Å)
HDB-1	95 ± 6	1.70 ± 0.02	1.03 ± 0.01	6.5 ± 0.5
HDB-2	103 ± 8	1.71 ± 0.02	1.04 ± 0.02	6.7 ± 0.4
HDB-3	104 ± 8	1.73 ± 0.02	1.05 ± 0.02	6.6 ± 0.5
HDB-4	79 ± 4	1.78 ± 0.04	1.08 ± 0.03	6.9 ± 0.5

a: S. Costeux, P. Wood-Adams, and D. Beigzadeh, Macromolecules **35**, 2514 (2002).

P. Wood-Adams, J. M. Dealy, Macromolecules **33**, 7481(2000).

P. Wood-Adams, J. M. Dealy, A. W. deGroot, O. D. Redwine, , Macromolecules **33**, 7489 (2000).

Branch content of metallocene polyethylene Ramachandran R, Beaucage G, Kulkarni AS, McFaddin D, Merrick-Mack J, Galiatsatos V *Macromolecules*, **42** 4746-4750 (2009).

Comparison of n_{Br} from SANS with β from NMR for Weakly Branched HDPE Samples

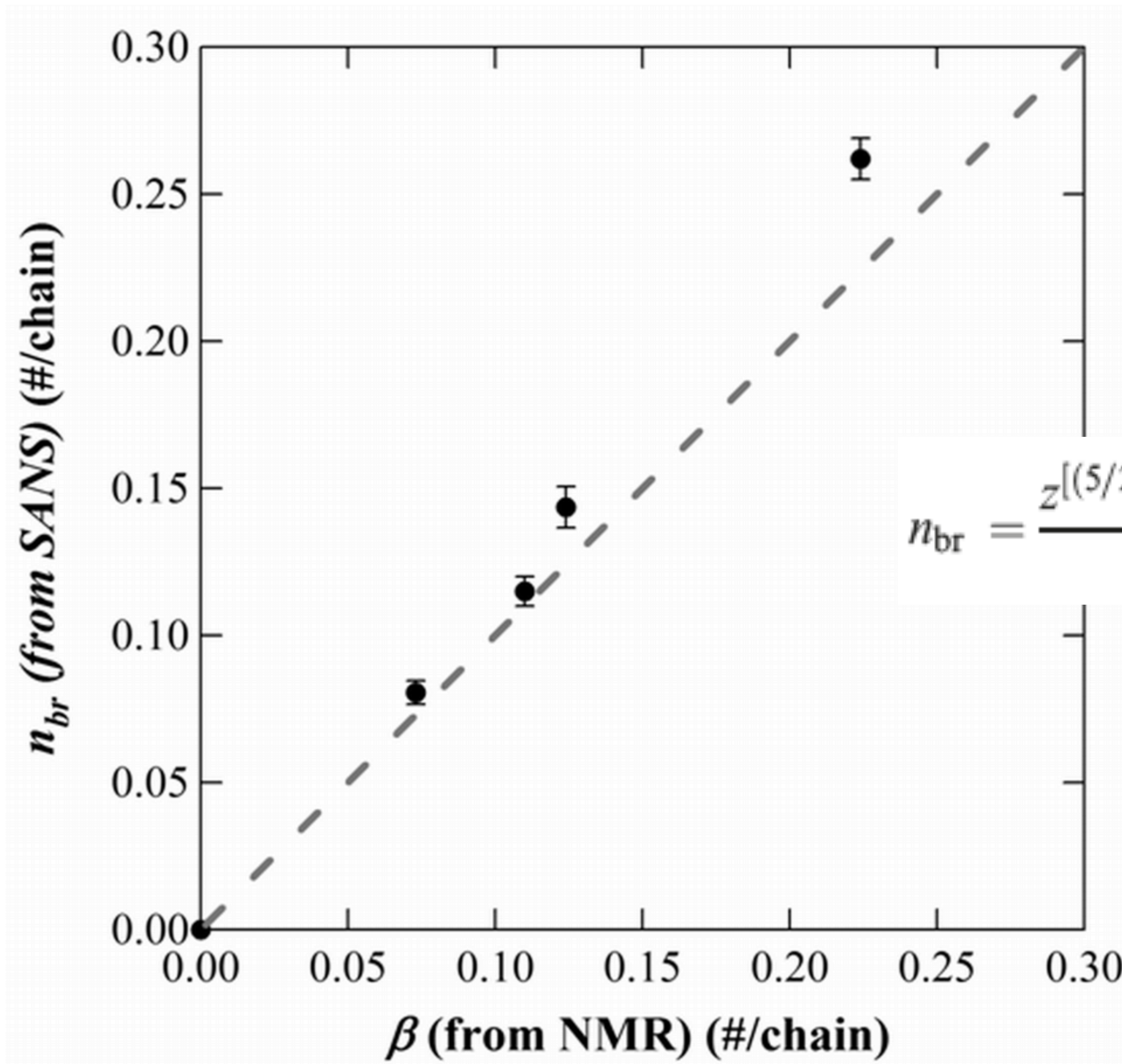

$$n_{br} = \frac{z^{[(5/2d_f) - (3/2c)] + [1 - (1/c)]} - 1}{2}$$

Branch content of metallocene polyethylene Ramachandran R, Beaucage G, Kulkarni AS, McFaddin D, Merrick-Mack J, Galiatsatos V *Macromolecules*, **42** 4746-4750 (2009).

S. Costeux, P. Wood-Adams, and D. Beigzadeh, Macromolecules **35**, 2514 (2002).

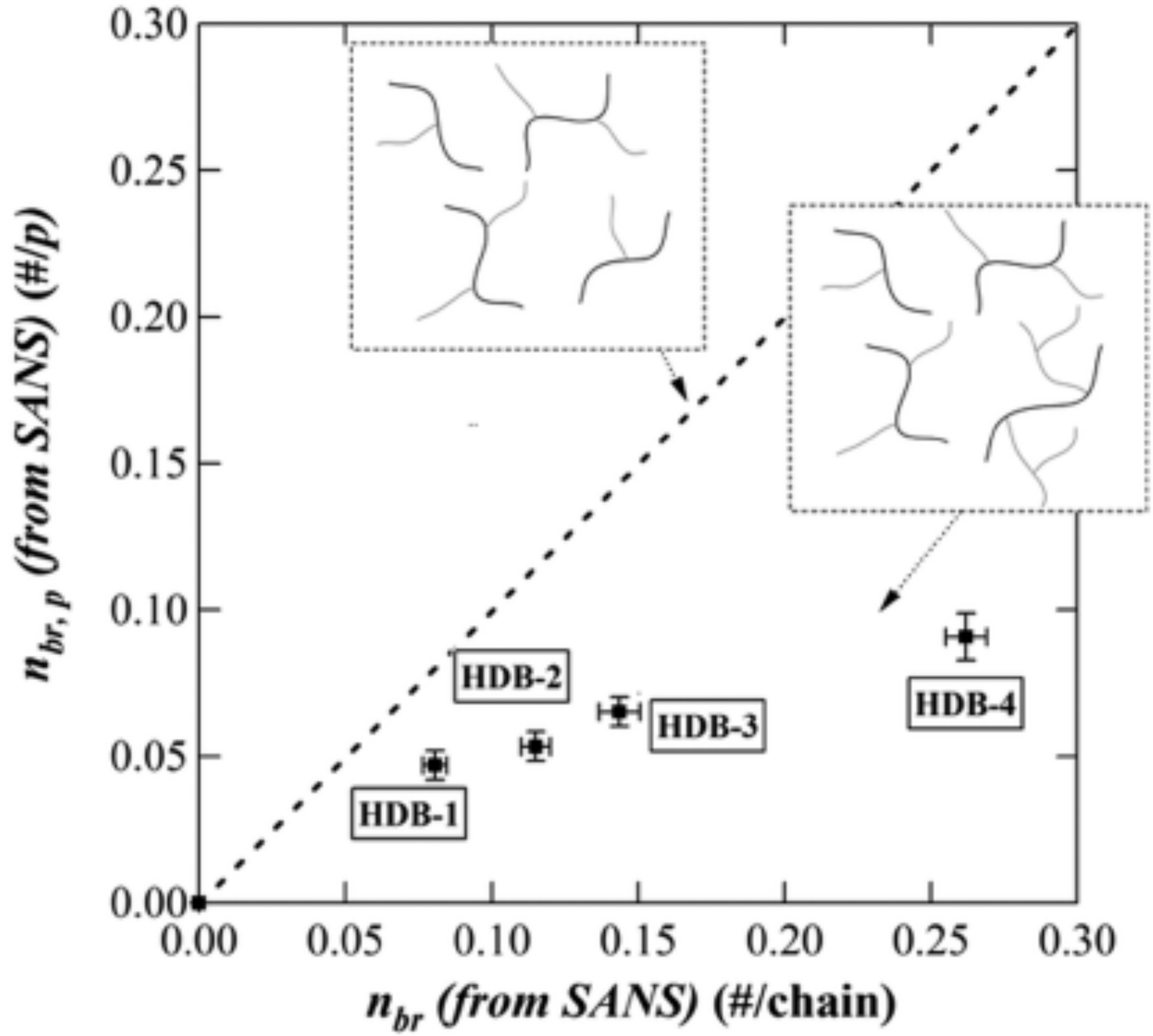

$$n_i = n_{br} - n_{br,p}$$

Branch content of metallocene polyethylene Ramachandran R, Beaucage G, Kulkarni AS, McFaddin D, Merrick-Mack J, Galiatsatos V *Macromolecules*, **42** 4746-4750 (2009).

Number of "inner" segments, n_i,
The effect of branch-on-branch structure

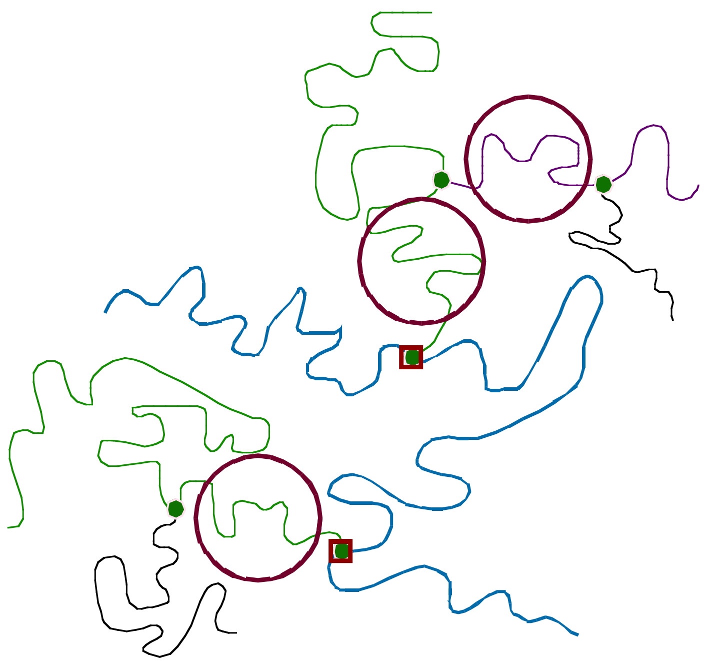

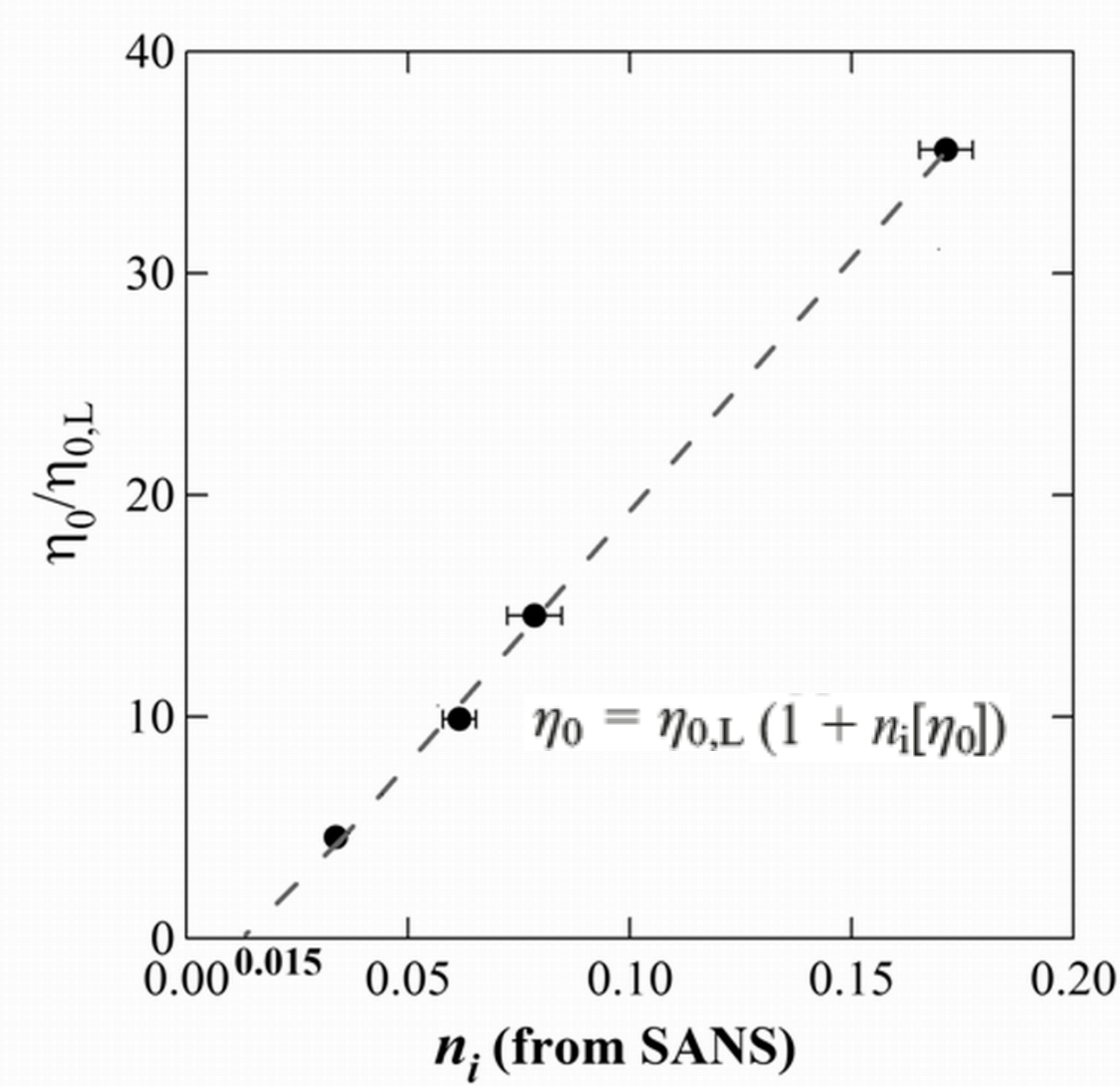

Branch content of metallocene polyethylene Ramachandran R, Beaucage G, Kulkarni AS, McFaddin D, Merrick-Mack J, Galiatsatos V *Macromolecules*, **42** 4746-4750 (2009).

The Effect of Branch Length, z_{br}, on Viscosity Enhancement for Weakly Branched HDPE Samples

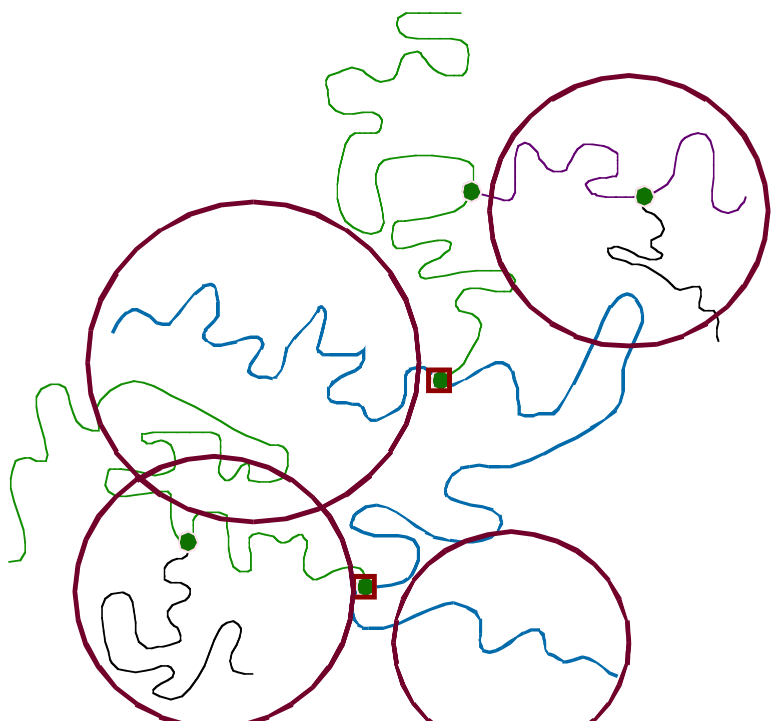

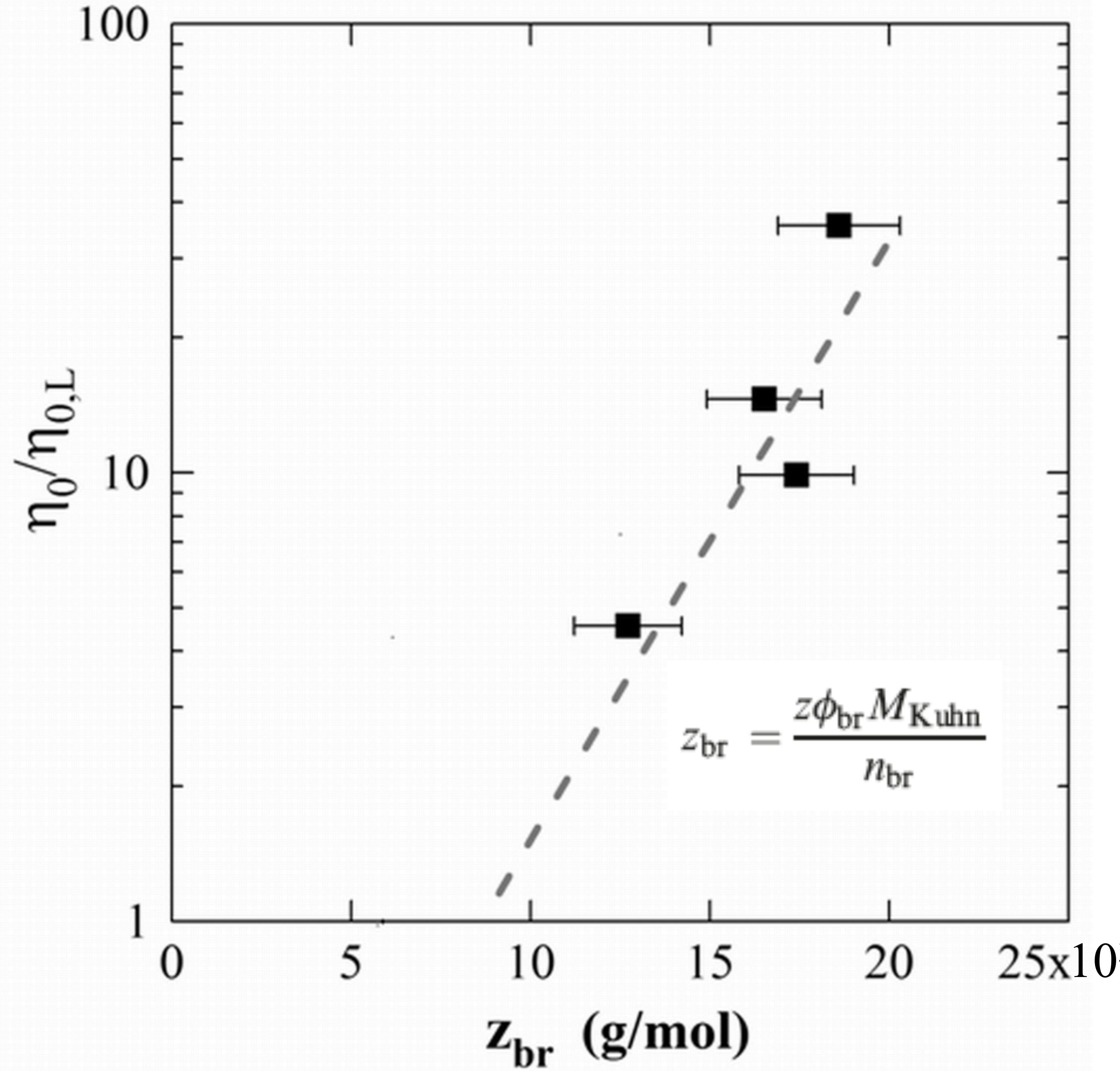

Branch content of metallocene polyethylene Ramachandran R, Beaucage G, Kulkarni AS, McFaddin D, Merrick-Mack J, Galiatsatos V *Macromolecules*, **42** 4746-4750 (2009).

The Effect of Branch Length, z_{br}, on Viscosity Enhancement for Weakly Branched HDPE Samples

For model (monodisperse) polymers entanglement effects are observed at*
$2.4\ M_e = 2.4 \times 1250$
$\langle z_{Br} \rangle_{n,1} = 3000$ g/mole
$\langle z_{Br} \rangle_{wt,1} = 9000$ g/mole

$PDI_{Br} \sim 3$

($PDI_{Chain} \sim 2$)

*Gell, C. B., Graessley, W. W., Efstratiadis V., Pitsikalis M., Hadjichristidis, N J. Polym. Sci. Part B **35**, 1943 (1997).*

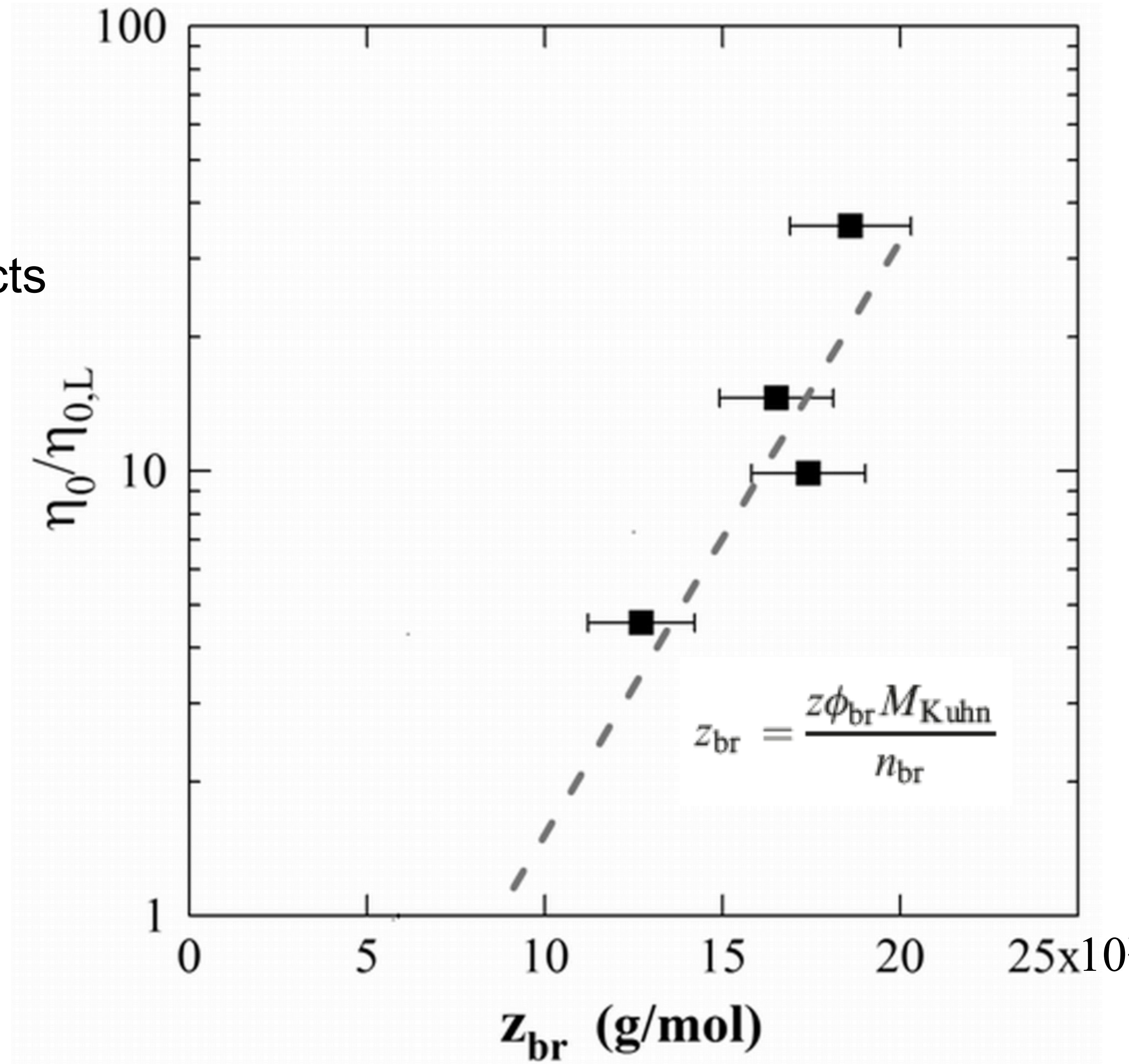

Branch content of metallocene polyethylene Ramachandran R, Beaucage G, Kulkarni AS, McFaddin D, Merrick-Mack J, Galiatsatos V *Macromolecules*, **42** 4746-4750 (2009).

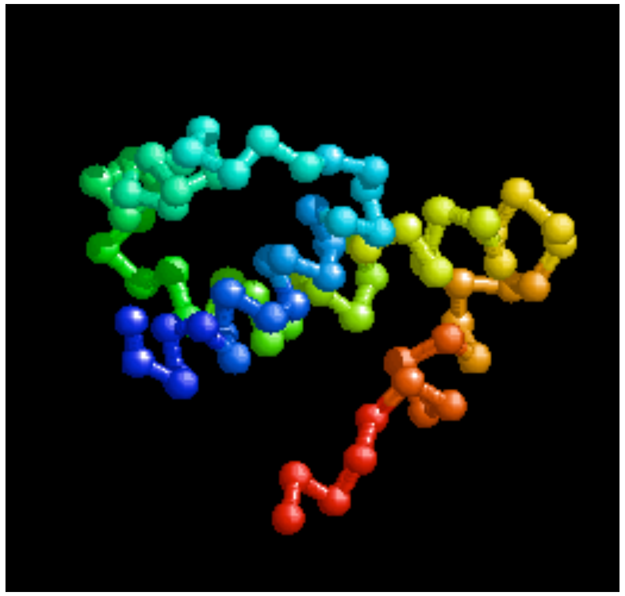

Quantification of the Macromolecular/ Nanoscale Topology using Small Angle Neutron and X-ray Scattering

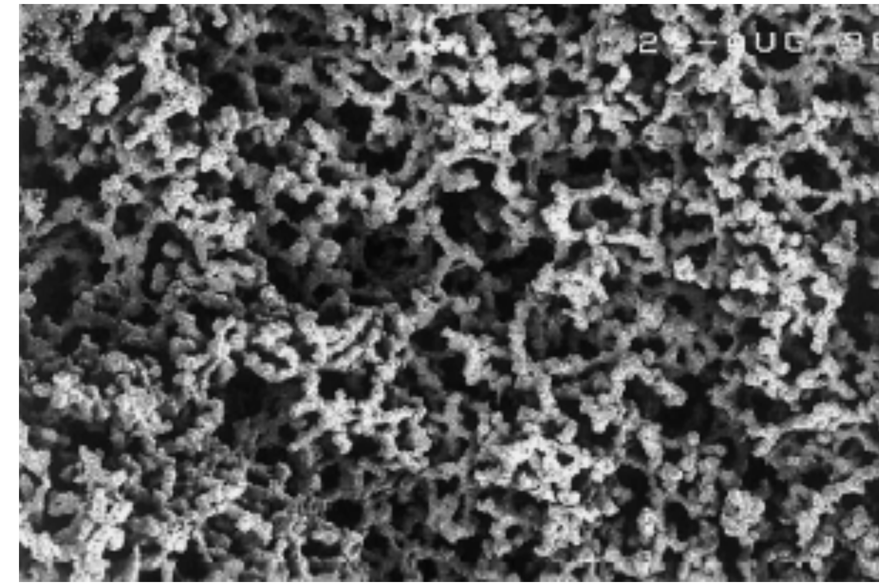

-A scaling model for complex topologies was presented.

-Decompose structure into *topological network* & *tortuous path*.

-Small-angle scattering can be used as an effective tool for determination of topology in complex hierarchical macromolecules.

-Use this information to construct molecular models & growth pathways.

-Method is applicable to a wide range of materials: Polymers, star molecules, cyclics, biomolecules, inorganic chain aggregates.

-Potential for broad understanding of complex hierarchical structures.

NSF, Swiss Commission for Technology and Innovation, LyondellBasell Industries

UNIVERSITY OF Cincinnati